Journal of Medicinal Chemistry

Discovery of Novel Schizocommunin Derivatives as Telomeric G-quadruplex Ligands that Trigger Telomere Dysfunction and the Deoxyribonucleic Acid (DNA) Damage Response

Tong Che, Shuo-Bin Chen, Jia-Li Tu, Bo Wang, Yu-Qing Wang, Yan Zhang, Jing Wang, Zeng-Qing Wang, Ze-Peng Zhang, Tian-Miao Ou, Yong Zhao, Jia-Heng Tan, and Zhi-Shu Huang

J. Med. Chem., **Just Accepted Manuscript** • DOI: 10.1021/acs.jmedchem.7b01615 • Publication Date (Web): 04 Apr 2018

Just Accepted

ACS Publications

is published by the American Chemical Society. 1155 Sixteenth Street N.W., Washington, DC 20036

Discovery of Novel Schizocommunin Derivatives as Telomeric G-quadruplex Ligands that Trigger Telomere Dysfunction and the Deoxyribonucleic Acid (DNA) Damage Response

Tong Che[a], Shuo-Bin Chen[a], Jia-Li Tu[a], Bo Wang[a], Yu-Qing Wang[a], Yan Zhang[a], Jing Wang[a], Zeng-Qing Wang[a], Ze-Peng Zhang[b], Tian-Miao Ou[a], Yong Zhao[b], Jia-Heng Tan[a,] *, and Zhi-Shu Huang[a,] *

[a] *Guangdong Provincial Key Laboratory of New Drug Design and Evaluation, School of Pharmaceutical Sciences, Sun Yat-sen University, Guangzhou, Guangzhou 510006, China*

[b] *School of Life Sciences, Sun Yat-sen University, Guangzhou 510006, People's Republic of China*

ABSTRACT

Telomeric G-quadruplex targeting and telomere maintenance interference are emerging as attractive strategies for anticancer therapies. Here, a novel molecular scaffold is explored for telomeric G-quadruplex targeting. A series of novel schizocommunin derivatives was designed and synthesized as potential telomeric G-quadruplex ligands. The interaction of telomeric G-quadruplex DNA with the derivatives was explored by biophysical assay. The cytotoxicity of the derivatives toward cancer cell lines was evaluated by the methyl thiazolyl tetrazolium (MTT) assay. Among the derivatives, compound **16** showed great stabilization ability toward telomeric G-quadruplex DNA and good cytotoxicity toward cancer cell lines. Further cellular experiments indicated that **16** could induce the formation of telomeric G-quadruplex in cells, triggering a DNA damage response at the telomere and causing telomere dysfunction. These effects ultimately provoked p53-mediated cell cycle arrest and apoptosis, and suppressed tumor growth in a mouse xenograft model. Our work provides a novel scaffold for the development of telomeric G-quadruplex ligands.

KEYWORDS

G-quadruplex; schizocommunin derivatives; interaction; telomere dysfunction; DNA damage

INTRODUCTION

Telomeres, located at the end of chromosomes, are essential for chromosome stability and genomic integrity.[1, 2] The telomere terminus is protected by a special lariat-like structure called the T-loop, which forms via strand invasion of 3′ single-stranded DNA into the duplex portion of the telomere and is further stabilized by shelterin, a six-subunit protein complex.[3-5] Uncapping of the telomere ends leads to telomeric dysfunction, characterized by end-to-end fusions and anaphase bridges, and triggers DNA damage responses that result in either senescence or apoptosis. This telomere maintenance plays a significant role in tumorigenesis and is crucial for the unlimited proliferative potential of cancer cells. Hence, disruption of telomere maintenance is considered an attractive strategy in anticancer therapy.[6, 7]

The 3′-terminal single-stranded DNA (TTAGGG repeats) prefers to fold into a four-stranded G-quadruplex structure,[8, 9] which can be detected by G-quadruplex antibodies in cells.[10] A number of studies have shown that telomeric G-quadruplex ligands might perturb telomere replication and cause telomere uncapping.[11-13] The stabilization of telomeric G-quadruplexes by these ligands can alter the T-loop structure, leading to its degradation through a DNA damage response pathway and the release of some shelterin proteins from the telomeres. Telomere dysfunction ultimately leads to cell cycle arrest, senescence, or apoptosis.[14-17] The development of telomeric G-quadruplex ligands as potential anticancer chemotherapy agents has become a popular research topic.[18-21]

To date, many studies have been performed seeking candidates for telomeric G-quadruplex ligands.[20] The characteristic telomeric G-quadruplex ligands usually have two characteristics: (i) a hetero-polyaromatic planar chromophore, which binds via π-π stacking to a terminal G-quartet and (ii)

one or more flexible substituents with a cationic charge to bind to quadruplex grooves and loops.[21-23]

Natural products are a prime source of innovative molecular fragments and are privileged scaffolds for drug discovery and development.[24] Several telomeric G-quadruplex ligands are derived from natural products, such as quindoline derivative **1** (SYUIQ-5),[25] bis-quinoline derivative **2** (PDS)[26] and acridine derivative **3** (BRACO-19)[11] (Figure 1). Schizocommunin (**4**, Figure 1) is a natural alkaloid that comprises a quinazoline moiety conjugated to an isatin group.[27, 28] X-ray crystallographic analysis of schizocommunin showed intramolecular hydrogen bonding between the hydrogen at N-3 and the oxygen at C-2′ (Figure S1).[28] The intramolecular hydrogen bond is an important structural factor that can rigidify molecules and maintain a large, nearly planar structure, which may allow ligands to effectively stack with the G-quartet.[29, 30] The crescent-shaped, large, nearly planar chromophore led us to explore a novel scaffold for the design of selective G-quadruplex ligands.

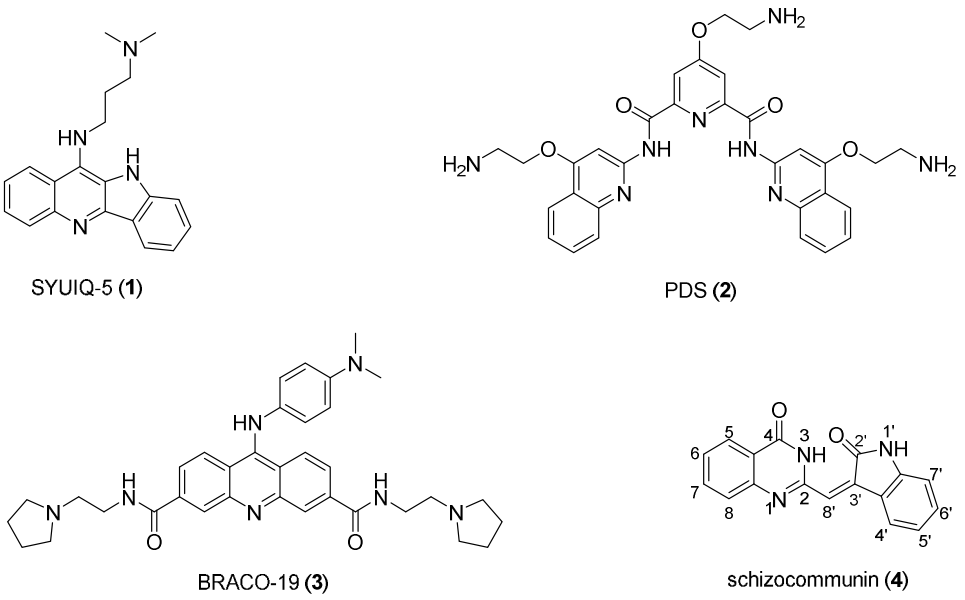

Figure 1. Chemical structures of G-quadruplex ligands **1**, **2**, **3**, and natural schizocommunin (**4**).

To explore new and selective G-quadruplex ligands for cancer chemotherapy, we designed and

synthesized a series of schizocommunin derivatives by attaching cationic amino side chains and introducing a fluorine atom into the aromatic chromophore. Fluorine atoms, with high electronegativity and small size, often exhibit unique properties in functional molecules.[31] The electron-withdrawing effect of fluorine could reduce the electron density of the aromatic chromophore, which might favor a stronger interaction with the electron-rich π-system of the G-quartet.[32] In addition, the introduction of fluorine atoms into small molecules might improve liposolubility and bioavailability. The structure-activity relationships and activity mechanism were also investigated. The results revealed that derivatives could selectivity stabilize and bind to the telomeric G-quadruplex *in vitro* and in cells. Further studies showed that our compound could trigger a DNA damage response at telomere regions and induce telomere uncapping, resulting in cell cycle arrest and apoptosis. Compound also inhibited tumor growth in a mouse xenograft model of cervical squamous cancer.

RESULTS AND DISCUSSION

Chemistry. The synthetic route for the derivatives is shown in Scheme 1. The preparation of the key intermediates, 2-methylquinazolin-4(*3H*)-one derivatives **3a - 3o**, was performed with commercially available 2-amino-4,5-difluorobenzoic acid (**1a**) or 2-amino-5-fluorobenzoic acid (**1b**) as the starting material through the synthesis of intermediates **2a - 2d** according to the reported method.[33, 34] Other key intermediates, isatin (indoline-2,3-dione) derivatives **6a - 6d**, were synthesized through the introduction of side chains onto intermediates **5a** or **5b**, which were prepared in a two-step cyclization reaction with the aniline substituent as the starting material, following reported procedures.[35] The isatin intermediates

6a - 6d were reacted with the prepared quinazolinone intermediates **3a - 3o** through a Claisen–Schmidt condensation and provided the target compounds **7 - 36**. Compound **37** was synthesized through a reaction of intermediate **3b** with 1-(3-(diethylamino)propyl)indoline-2,3-dione (**6e**), which was prepared with bromide **5d** using isatin (**5c**) as the starting material.[36] The structures of the schizocommunin derivatives **7 - 37** are shown in Table 1. The E configuration of the exocyclic double bond of compounds **35** and **36** was identified using nuclear overhauser effect (NOE) spectroscopy (Figure S2). The Z configuration of the double bond of other molecules (**7 - 34**, **37**) was confirmed by ^{1}H NMR, showing the chemical shift of the hydrogen at N-3 in the molecules was approximately 14 ppm. Such data clearly revealed the existence of hydrogen bonding between the hydrogen at N-3 and the oxygen at C-2′.

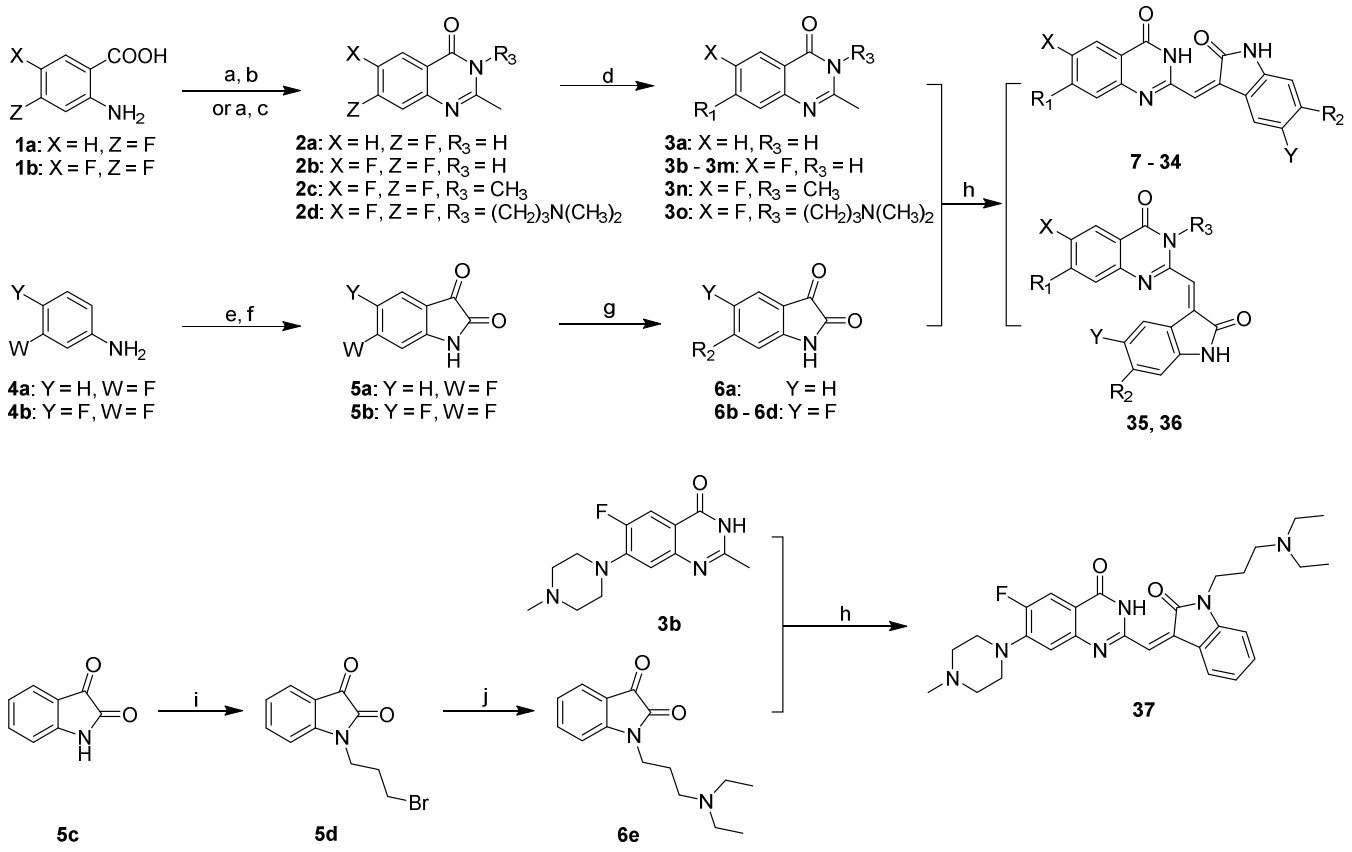

Scheme 1. Synthesis of schizocommunin derivatives **7 - 37**. Reagents and conditions: (a) acetic anhydride, 120 °C, 2 h;

(b) 25% $NH_3 \cdot H_2O$, reflux, 2 h; (c) amine, r.t; (d) CH_3CN, reflux; (e) NH_2OH/HCl, $Cl_3CCH(OH)_2$; (f) 98% H_2SO_4; (g) CH_3CN, r.t; (h) acetic acid, reflux; (i) 60%NaH, 1,3-dibromopropane, rt; and (j) ethylenediamine, rt.

Table 1. Structures of the newly synthesized schizocommunin derivatives (**7 - 36**).

Compd.	X	Y	R_1	R_2	R_3	Compd.	X	Y	R_1	R_2	R_3
7	H	H	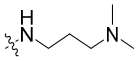	H	H	**22**	F	F	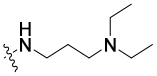		H
8	F	H	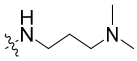	H	H	**23**	F	F	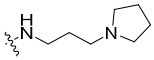		H
9	F	H	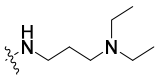	H	H	**24**	F	F	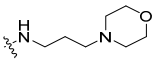		H
10	F	H	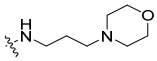	H	H	**25**	F	F	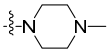		H
11	F	H	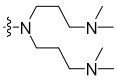	H	H	**26**	F	F	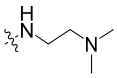	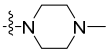	H
12	H	H	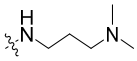	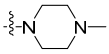	H	**27**	F	F	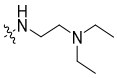	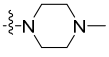	H
13	F	H	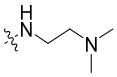	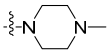	H	**28**	F	F	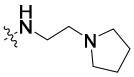	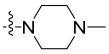	H
14	F	H	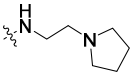	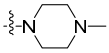	H	**29**	F	F	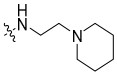	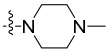	H
15	F	H	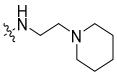	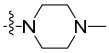	H	**30**	F	F	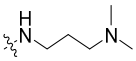	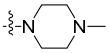	H
16	F	H	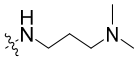	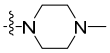	H	**31**	F	F	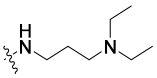	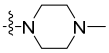	H
17	F	H	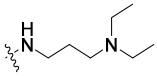	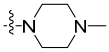	H	**32**	F	F	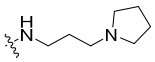	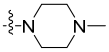	H
18	F	F	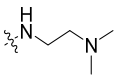	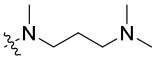	H	**33**	F	F	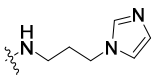	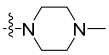	H
19	F	F	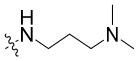	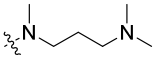	H	**34**	F	F	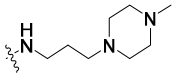	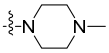	H
20	F	F	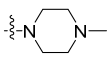	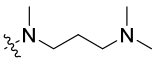	H	**35**	F	H	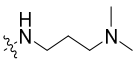	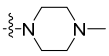	CH_3

21	F	F	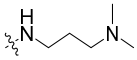		H	**36**	F	H	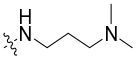	H	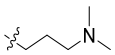

Interacting ability and selectivity of derivatives with telomeric G-quadruplex DNA over duplex DNA. To evaluate the stabilization of schizocommunin derivatives for telomeric G-quadruplex DNA, fluorescence resonance energy transfer (FRET) melting experiments were performed, and the quindoline derivative **1** previously reported by us was used as a reference compound.[25, 37-40] F21T (5′-*FAM*-d(GGG[TTAGGG]$_3$)-*TAMRA*-3′) represents the human telomeric DNA sequence, while F10T (5′-*FAM*-d(TATAGCTATA-HEG-TATAGCTATA)-*TAMRA*-3′, with an hexaethylene glycol (HEG) linker of [(-CH_2-CH_2-O-)$_6$]), is a hairpin duplex DNA (Table S1). The effect of the derivatives on the enhanced melting temperature (ΔT_m) of the two labeled oligonucleotides in a K^+ solution is shown in Table 2, and all original melting curves are shown in Figures S3-S5. The FRET melting data demonstrated that most derivatives effectively stabilized the telomeric G-quadruplex F21T (ΔT_m >10 °C) and that their stabilization ability was better than for compound **1** (ΔT_m = 11.6 °C), while no compounds were observed to significantly increase the stability of the duplex DNA F10T (ΔT_m <1 °C) (Table 2). The structure-activity relationship was further explored as described below.

First, the number of alkylamino side chains had a significant impact on stabilization activity. Compounds with two alkylamino side chains, such as **12**, **16**, and **17**, showed a dramatically increased stabilization ability with the telomeric G-quadruplex compared to compounds **7**, **8**, and **9** with one alkylamino side chain. In addition, the length and type of alkylamino side chain were also important factors for the stabilization activity of the tested compounds. At the 6′-position, compounds with an

N-methyl piperazino group (**30**, **31**, and **32**) showed stronger stabilization activity for the G-quadruplex than the morpholino group (**21**, **22**, and **23**) and the *N, N, N′*-trimethylpropane-1,3-diamino group (**19**). At the 7-position, compounds **16**, **30**, and **31**, with n = 3 and a dimethylamino or diethylamino terminus, appeared to be more potent in the stabilization of the G-quadruplex structure than compounds with a shorter chain (n = 2, compounds **13**, **26**, **27**). When the length of the side chain at the 7-position was the same, compounds with a dimethylamino or diethylamino terminus (monofluoro series: **13**, **16**, and **17**; difluoro series: **30**, and **31**) showed the most potent activity.

Table 2. Stabilization temperatures (ΔT_m) determined by FRET and equilibrium binding constants (K_D) determined by SPR.

Compd.	ΔT_m (°C)[a]		K_D (M)[b]		Compd.	ΔT_m (°C)[a]		K_D (M)[b]	
	F21T	F10T	HTG21	Duplex		F21T	F10T	HTG21	Duplex
7	8.4	0.1	$> 4.0\times10^{-5}$	–	**23**	8.4	0.3	$> 4.0\times10^{-5}$	–
8	11.8	0.2	$> 4.0\times10^{-5}$	–	**24**	5.2	0.2	$> 4.0\times10^{-5}$	–
9	10.0	0.1	$> 4.0\times10^{-5}$	–	**25**	12.2	0.1	$> 4.0\times10^{-5}$	–
10	8.6	0.1	$> 4.0\times10^{-5}$	–	**26**	22.5	0.3	6.2×10^{-6}	1.5×10^{-5}
11	12.6	0.2	2.3×10^{-5}	–	**27**	23.1	0.3	2.2×10^{-5}	–
12	16.5	0.1	$> 4.0\times10^{-5}$	–	**28**	22.7	0.1	2.1×10^{-5}	–
13	18.0	0.2	$> 4.0\times10^{-5}$	–	**29**	21.4	0.2	8.8×10^{-6}	1.6×10^{-5}
14	18.6	0.2	$> 4.0\times10^{-5}$	–	**30**	24.6	0.1	7.6×10^{-6}	–
15	18.7	0.2	$> 4.0\times10^{-5}$	–	**31**	25.3	0.1	4.9×10^{-6}	–

16	23.5	0.1	8.1×10^{-6}	−	**32**	23.6	0.3	7.9×10^{-6}	−
17	20.6	0.2	7.4×10^{-6}	−	**33**	11.5	0.5	2.1×10^{-5}	−
18	20.1	0.3	1.4×10^{-5}	−	**34**	19.8	0.1	9.6×10^{-6}	−
19	18.2	0.3	1.8×10^{-5}	−	**35**	7.4	0.1	3.0×10^{-5}	$> 4.0\times10^{-5}$
20	15.6	0.2	$> 4.0\times10^{-5}$	−	**36**	9.2	0.1	$> 4.0\times10^{-5}$	−
21	11.9	0.1	$> 4.0\times10^{-5}$	−	**37**	5.8	0.3	$> 4.0\times10^{-5}$	−
22	9.0	0.1	$> 4.0\times10^{-5}$	−	**1**	11.6	5.2	nd	nd

[a] $\Delta T_m = T_m$ (DNA + ligand) - T_m (DNA). ΔT_m values for the incubation of 0.2 μM F21T or F10T with and without 1.0 μM of the compound in Tris-HCl buffer (10 mM, pH 7.4) containing 60 mM KCl. In the absence of a ligand, the T_m values of annealed F21T and F10T are 60 and 61 °C, respectively. [b] K_D for compounds toward HTG21 and hairpin sequence as determined using SPR. Compounds that did not achieve saturation state at the highest tested concentration (40 μM) are noted as $> 4.0 \times 10^{-5}$ M. Compounds that did not achieve significant binding signal at the highest tested concentration (40 μM) are noted as −. nd: Not determined

Second, the introduction of a fluorine atom at the 6-position of the schizocommunin ring system, such as in compounds **8** and **16**, could increase the stabilization ability of the compounds bound to the G-quadruplex DNA compared to compounds **7** and **12** without fluorine atoms. Furthermore, when the second fluorine atom was added at the 5′-position of the moiety, such as in difluoro-compounds **26**, **28**, **29**, **30**, and **31**, the ΔT_m values were further increased over the corresponding monofluoro-compounds **13**, **14**, **15**, **16**, and **17**.

To investigate the effect of the aromatic chromophore on activity, the introduction of a methyl group (**35**) or alkylamino side chain (**36**) at the 3-position showed an obvious decrease in stabilizing activity (Table 2 and Figure S4). Compound **37** with two alkylamino side chains at the 1′- and 7-positions also showed poor stabilizing activity (Table 2 and Figure S5). These results indicate that the scaffold of

schizocommunin and the direction of the alkylamino side chain are crucial for telomeric G-quadruplex stabilization.

To confirm the selectivity of the derivatives for the G-quadruplex DNA over duplex DNA, a FRET-based competition assay was performed.[41] The ability of the ligands to retain the G-quadruplex stabilizing affinity was challenged with non-fluorescent duplex DNA ds26 (5′-GTTAGCCTAGCTTAAGCTAGG-CTAAC-3′). As shown in Figure 2, in the presence of excess competitor ds26, the thermal stabilization of F21T, which was enhanced by compounds **7**, **16** and **30**, was slightly affected, while the competitor sharply disrupted the binding of reference compound **1** to the G-quadruplex. These results demonstrated that schizocommunin derivatives could specifically stabilize the telomeric G-quadruplex over duplex DNA.

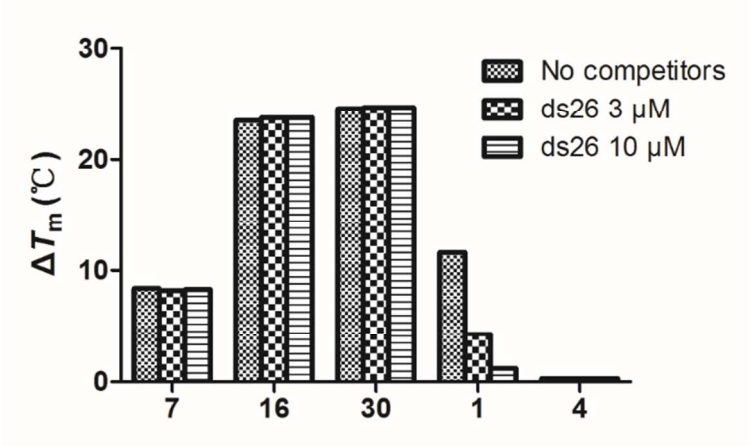

Figure 2. Competitive FRET results for derivatives with or without a 15-fold (3 μM) and 50-fold (10 μM) excess of the duplex DNA competitor (ds26). The concentration of F21T was 0.2 μM, and the concentration of the tested compounds was 1 μM. For the experiments, 10 mM Tris-HCl buffer (pH 7.4) containing 60 mM KCl was used.

Considering the effect of fluorophores in the FRET experiments, a circular dichroism (CD) melting assay was performed to confirm the stabilization activity. As shown in Table S2, the results were similar

to the structure-activity relationship (SAR) analysis in the FRET experiments. To further investigate the interaction between compounds and other G-quadruplexes, CD melting assay with different G-quadruplex DNAs was also explored. As shown in Table S3 and Figure S6, the results showed that compound **16** was effective at stabilizing telomeric G-quadruplex. It could also stabilize other G-quadruplex DNAs in some extent.

To investigate the binding affinity of the derivatives for the telomeric G-quadruplex, a surface plasmon resonance (SPR) assay was employed.[42] The binding affinities (K_D) were determined through equilibrium analysis, as shown in Table 2, and the SPR sensorgrams and fits were shown in Figures S7-S8. Similar to the FRET assay, the compounds (**16**, **30**, **31**) with the highest potential stabilizing activity showed the strongest binding affinity, with K_D values of ~10^{-6} M, while no obvious binding was found for the compounds to duplex DNA. The binding affinity various G-quadruplex DNAs was also explored by employing compound **16**. The results were consistent with CD melting assay that **16** was effective at binding with telomeric G-quadruplex and could also bind with other G-quadruplex DNAs in some extent (Table S4).

Taken together, the derivatives with the *N,N*-dimethylamino propylamino or *N,N*-diethylamino propylamino group at the 7-position and the *N*-methyl piperazino group at the 6′-position showed the best stabilization activity and binding affinity for the telomeric G-quadruplex.

Cytotoxicity activities of the derivatives. The above results show that the derivatives have a high binding affinity for telomeric G-quadruplexes, thus having the potential to act as a favorable antitumor agent by disturbing telomere maintenance. To identify effective G-quadruplex ligands with

antitumor activity, an MTT assay to evaluate cytotoxicity was performed.[43] All derivatives were evaluated for cytotoxicity activities against four telomerase-positive cancer cell lines, the human cervical cancer cell line (HeLa), the human cervical squamous cancer cell line (SiHa), the human acute leukemia cell line (HL-60), and the adenocarcinomic human alveolar basal epithelial cancer cell line (A549), and a telomerase-negative cell line, the alternative lengthening of telomeres (ALT) human osteosarcoma cell line (U2OS) for further exploring of action mechanism of compounds.

Table 3. IC_{50} values (μM) of schizocommunin derivatives against tumor cells by the MTT assay[a].

Compd.	IC_{50} (μM)					Compd.	IC_{50} (μM)				
	HeLa	SiHa	HL60	A549	U2OS		HeLa	SiHa	HL60	A549	U2OS
7	42.5	27.6	4.1	19.6	20.4	**23**	> 50	42.5	3.8	> 50	> 50
8	13.4	17.1	3.2	14.8	18.7	**24**	> 50	> 50	> 50	> 50	> 50
9	> 50	23.4	7.5	8.6	12.6	**25**	> 50	> 50	12.3	> 50	> 50
10	> 50	> 50	> 50	> 50	> 50	**26**	7.7	11.4	2.8	6.0	5.7
11	48.6	10.1	16.1	> 50	> 50	**27**	9.0	12.4	1.7	6.1	8.2
12	49.0	11.5	4.3	19.0	14.1	**28**	10.5	9.3	2.7	5.6	7.1
13	15.7	3.4	7.8	2.2	6.3	**29**	2.8	4.4	2.9	1.4	5.3
14	17.4	10.9	3.6	4.1	6.4	**30**	17.6	4.9	3.8	5.9	9.0
15	20.5	5.4	2.8	1.8	3.6	**31**	9.6	7.9	5.7	6.1	10.2

16	3.8	2.8	2.5	9.1	3.2	**32**	9.0	9.4	2.9	25.3	16.4
17	10.0	2.8	5.4	2.3	7.6	**33**	> 50	> 50	> 50	> 50	> 50
18	22.6	7.6	5.6	12.4	9.2	**34**	8.8	2.8	3.3	9.7	12.7
19	7.1	2.9	6.5	14.3	8.3	**35**	14.0	14.0	30.6	15.4	12.5
20	12.8	3.5	3.2	10.4	9.4	**36**	27.1	30.5	8.2	18.2	28.4
21	30.1	> 50	3.4	> 50	> 50	**37**	> 50	> 50	13.2	> 50	> 50
22	34.3	43.6	4.2	> 50	32.4						

[a] All substances were evaluated for antiproliferative activities against the human acute leukemia cell line (HL-60), adenocarcinomic human alveolar basal epithelial cancer cell line (A549), human cervical cancer cell line (HeLa), human cervical squamous cancer cell line (SiHa), and telomerase-negative ALT human osteosarcoma cell line (U2OS) using the MTT assay, as described by Mosmann with modifications.

The cytotoxicity of the schizocommunin derivatives is shown as IC_{50} values (concentration for 50% inhibition) in Table 3. The results showed that most derivatives displayed significant cytotoxicity activities with low micromolar IC_{50} values. Compounds **13-19**, **26-32,** and **34** with stronger stabilizing activity for the G-quadruplex displayed better cytotoxicity activity against cancer cell lines.

Telomerase inhibition. The stabilization of the telomeric G-quadruplex is typically considered to inhibit telomerase activity. A modified telomeric repeat amplification protocol (TRAP) assay, the TRAP-LIG assay,[44] was performed to evaluate the telomerase inhibition activities of three representative derivatives, **7** with weak stabilizing and binding G-quadruplex ability and weak cytotoxicity, **16** with strong stabilizing and binding G-quadruplex ability, good selectivity against duplex DNA, and good cytotoxicity, and **30** with the highest stabilizing and strong binding G-quadruplex ability, and no bad

cytotoxicity. Considering that the presence of the compounds in the extended products may interfere with the PCR step, the ligands were removed prior to the amplification step.[45, 46] The results show that compound **16** has a potent inhibitory effect, with an inhibitory concentrations by the half ($^{Tel}IC_{50}$) value of 9.6 μM, better than that of compounds **30** ($^{Tel}IC_{50}$ = 12.3 μM) and **7** ($^{Tel}IC_{50}$ > 40 μM) (Figure S9).

Among all schizocommunin derivatives, compound **16** showed a good telomerase inhibitory effect, strong telomeric G-quadruplex stabilizing and binding ability, good selectivity over duplex DNA, and also a strong antiproliferative activity against the cancer cell lines. Thus, **16** was selected for further biological studies.

Stabilization and induction of the formation of telomeric G-quadruplex DNA by compound 16 in cells. To demonstrate whether compound **16** could stabilize the telomeric G-quadruplex in cancer cells, nuclear G-quadruplex structures in SiHa cells (Figure 3A-C) and U2OS cells (Figure S10A-C) were visualized using an immunofluorescence assay with the BG4 antibody, a known specific antibody against the G-quadruplex.[10] Compound **7** was used as a control.

As shown in Figure 3A-B and Figure S10A-B, the representative immunofluorescence images of SiHa cells and U2OS cells showed that **16** could induce a significant increase in BG4 foci in the nucleus, while compound **7** with poor stabilization activity toward telomeric G-quadruplex showed no significant change. Multiple cells image of BG4 foci in SiHa cells was showed in Figure S11. To further track whether the increase of BG4 foci was located at the telomere region, double immunofluorescence experiments using BG4 and the telomeric repeat binding factors 2 (TRF2) antibody, a specific antibody against the telomere binding protein TRF2, were performed to visualize the G-quadruplex and telomeres,

respectively. Figures 3A, 3C, and S9A showed that after treatment with **16**, the amount of BG4/TRF2 co-localized foci considerably increased compared to the untreated cells in both SiHa and U2OS cells, indicating the formation of a telomeric G-quadruplex. Notably, excluding some background BG4 foci, there's still a portion of **16**-induced BG4 foci that did not belong to telomeric G-quadruplexes. Indeed, a recent study that used a G-quadruplex chromatin immunoprecipitation sequencing (ChIP-seq) protocol employing BG4 revealed that an altered cellular state would cause a concomitant shift in the G-quadruplex profile in cells.[47] We speculated that, to some extent, **16** altered the cell status and then might change the G-quadruplex landscape in cells.

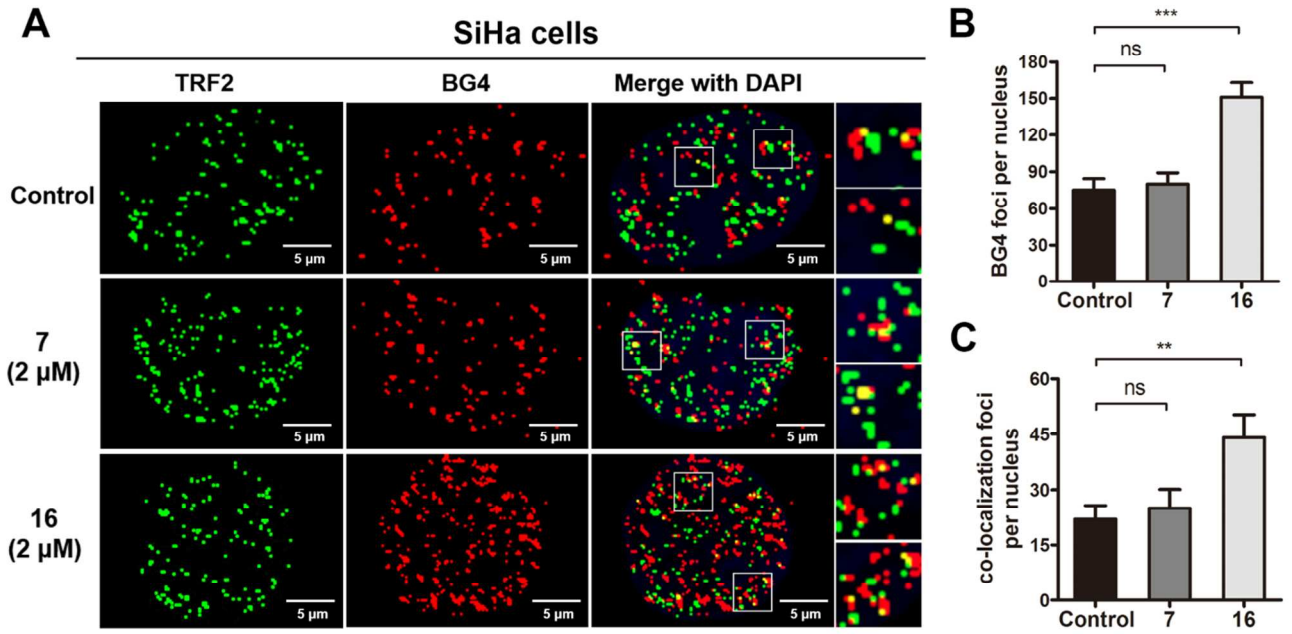

Figure 3. Compound **16** stabilized and induced the formation of telomeric G-quadruplexes in SiHa cells. (A) Representative immunofluorescence images of TRF2 (green) and BG4 (red) foci in SiHa cells treated with 2 μM **7**, 2 μM **16** or 0.1% dimethylsulfoxide (DMSO) (control) for 24 h. Nuclei were stained with 4',6-diamidino-2-phenylindole (DAPI) (blue). (B) Quantification of the number of BG4 foci per nucleus in SiHa cells. (C) Quantification of the

co-localization of BG4 and TRF2 per nucleus in SiHa cells. Two-tailed unpaired Student's t tests were applied for statistical analysis. The data were expressed as the mean ± standard error of mean (SEM): (∗) $P < 0.05$, (∗∗) $P < 0.01$, and (∗∗∗) $P < 0.001$, significantly different from the control. (ns) Not significantly different from the control.

Triggering of a DNA damage response at telomeres by compound 16. Compound **16** displayed comparable cytotoxicity in both telomerase-positive cancer cells and in telomerase-negative ALT cells (U2OS) (Table 3), suggesting that the cytotoxicity of **16** was not solely attributed to the telomerase inhibition but also due to some other pathways, such as activation of the telomeric DNA damage response.[16] As reported previously, the stabilization of telomeric G-quadruplexes by ligands can alter the T-loop structure, and the unprotected chromosome ends can be recognized and repaired as double-strand breaks (DSBs) to trigger DNA damage responses.[26] Moreover, uncapped telomeres can suffer degradation, inappropriate recombination, and end-to-end fusions, and this telomere dysfunction can lead to an effect similar to that of DNA damage in eliciting cell cycle arrest and apoptosis.[14]

To investigate whether treatment with compound **16** would induce the DNA-damage response, immunofluorescence experiments were performed. As shown in Figures 4A-B and S12, a significant increase in the histone H2A.X (γ-H2AX) foci (a characteristic of a DNA double strand break response) was observed after treatment with 2 μM **16** for 24 h, but no significant change was observed in the **7**-treated cells. To verify whether γ-H2AX was activated at the telomeres, double immunofluorescence experiments were further performed. The result showed that most γ-H2AX foci induced by **16** could co-localize with the TRF2 protein (Figure 4C), forming the so-called telomere dysfunction-induced foci (TIFs).[48] This result indicated that **16** triggered the DNA damage response at the telomeric region.

What's more, the increase of γ-H2AX foci (3-fold) was more than telomeric BG4 foci (2-fold), which might cause by other G-quadruplexes. A similar results was also observed in **16**-treated telomerase-negative ALT U2OS cells (Figure S13A-C), which indicated that compound **16** could also stabilize the structure of the telomeric G-quadruplex and induce the DNA-damage response of the telomeric region in U2OS cells. Furthermore, to investigate whether the telomeric DNA damage was induced by ligand binding to and stabilizing telomeric G-quadruplexes, we again performed double immunofluorescence experiments to stain both BG4 and γ-H2AX in SiHa cells. As shown in Figure S14, treatment with **16** significantly increased both BG4 and γ-H2AX foci, and the induced γ-H2AX foci co-localized with BG4 foci, suggesting that **16** could bind to and stabilize telomeric G-quadruplexes and then trigger DNA damage reponse.

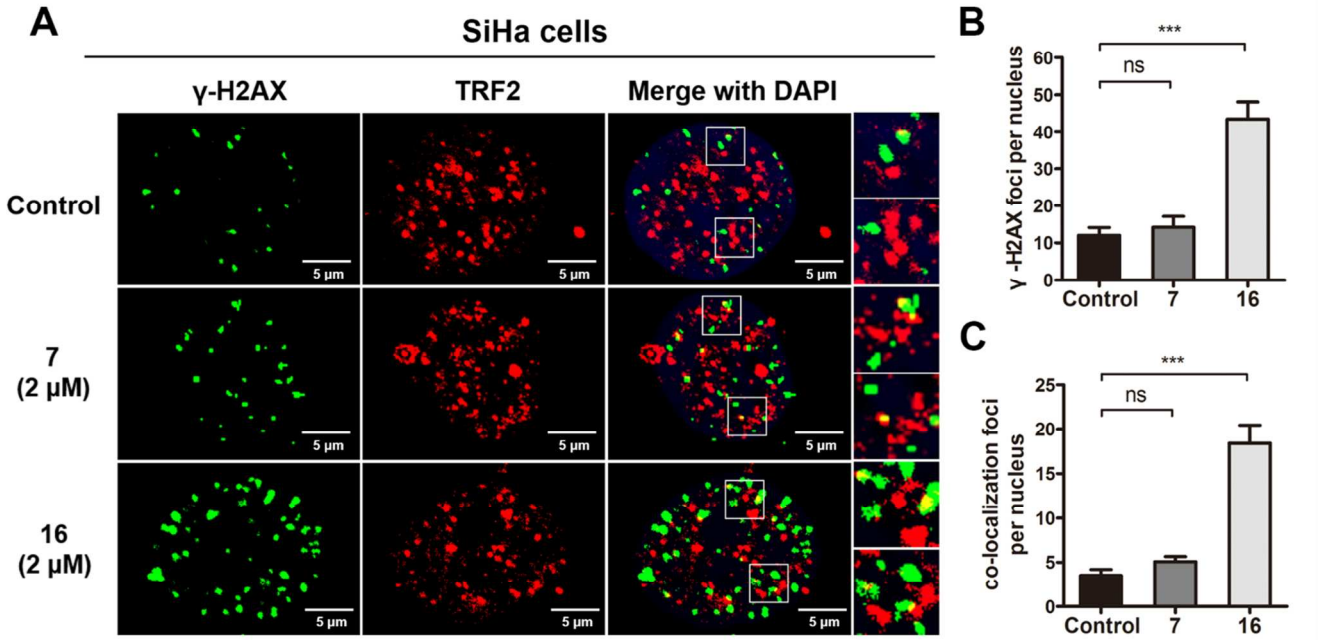

Figure 4. Compound **16** induced telomeric DNA damage in SiHa ells. (A) Representative immunofluorescence images of γ-H2AX (green) and TRF2 (red) foci in SiHa cells treated with 2 μM **7**, 2 μM **16** or 0.1% DMSO (control) for 24 h.

Nuclei were stained with DAPI (blue). (B) Quantification of the number of γ-H2AX foci per nucleus in SiHa cells. (C) Quantification of the co-localization of γ-H2AX and TRF2 per nucleus in SiHa cells. Two-tailed unpaired Student's t tests were applied for statistical analysis. The data were expressed as the mean ± SEM: (∗) $P < 0.05$, (∗∗) $P < 0.01$, and (∗∗∗) $P < 0.001$, significantly different from the control. (ns) Not significantly different from the control.

Induction of telomere-binding proteins dissociating and telomere uncapping by compound 16. The stabilization of the telomeric G-quadruplex might result in telomere dysfunction, characterized by the dissociation of the telomere binding protein, telomere uncapping and anaphase bridges.[26, 49] Next, the effects of compound **16** on the dissociation of telomere-binding proteins were investigated, with compound **7** as a control. Protection of telomeres 1 (POT1) binds to telomeric single-stranded DNA and regulates potential G-quadruplex structures formed at the telomeric G-overhang. It was reported that telomeric G-quadruplex stabilizers could delocalize POT1 from the telomeric region. Double immunofluorescence experiments showed that **16** significantly delocalized POT1 from TRF2 foci after 24 h of treatment (Figure 5A). Quantitative analysis of the number of POT1/TRF2 co-localized foci revealed an obvious reduction (Figure 5B). The western blot experiment further confirmed that the removal of POT1 from the telomeres was not associated with a change in its expression (Figure S15).

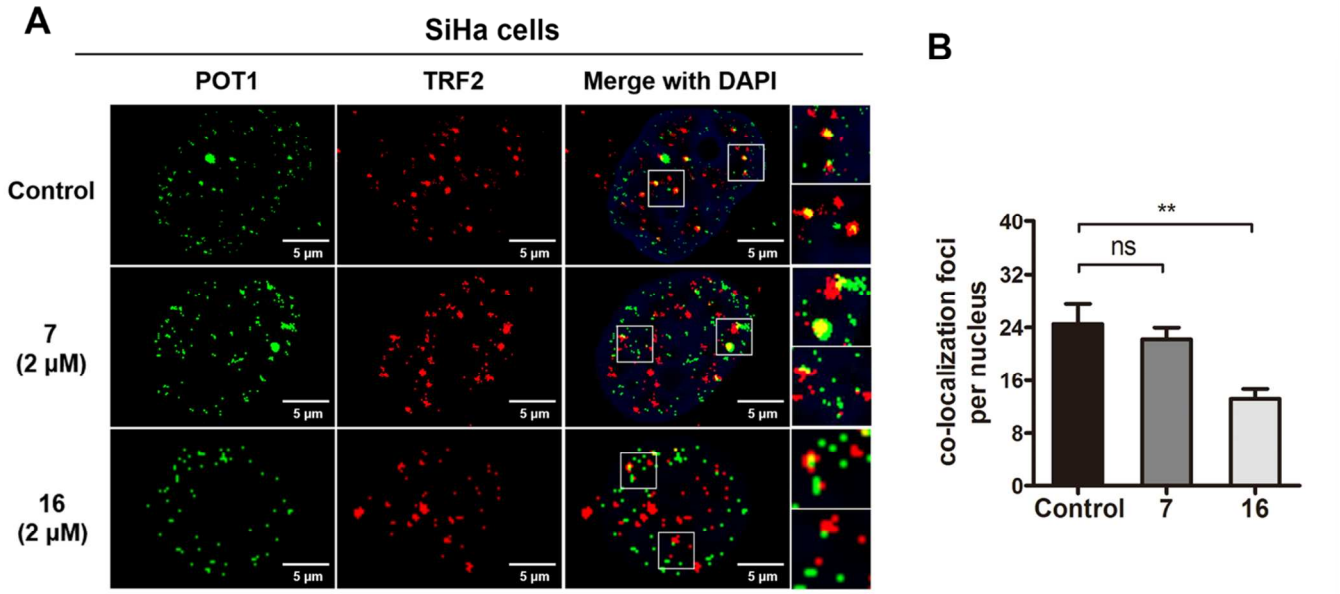

Figure 5. Compound 16 induced the dissociation of telomere-binding protein POT1. (A) Representative immunofluorescence images of POT1 (green) and TRF2 (red) foci in SiHa cells treated with 2 μM **7**, 2 μM **16** or 0.1% DMSO (control) for 24 h. Nuclei were stained with DAPI (blue). (B) Quantification of the co-localization of POT1 and TRF2 per nucleus in SiHa cells. Two-tailed unpaired Student's t tests were applied for statistical analysis. The data were expressed as the mean ± SEM: (∗) $P < 0.05$, (∗∗) $P < 0.01$, and (∗∗∗) $P < 0.001$, significantly different from the control. (ns) Not significantly different from the control.

It was reported that POT1 could suppress the activity of kinases in ataxia telangiectasia and Rad3-related (ATR) pathway at telomeres and that the removal of POT1 from telomeric overhangs might activate an ATR-dependent DNA damage response.[50] We further examined the ATR-related DNA damage and repair pathway using a western blot assay. As shown in Figure 6A, SiHa cells treated with compound **16** for 48 h induced a dose-dependent increase in phosphorylated ATR (p-ATR) and phosphorylated checkpoint kinase 1 (p-CHK1) to further increase the expression of phosphorylated P53

(p-P53). These findings indicate that DNA damage and repair occurred, with the up regulation of p-ATR, which might be related to the delocalization of POT1.

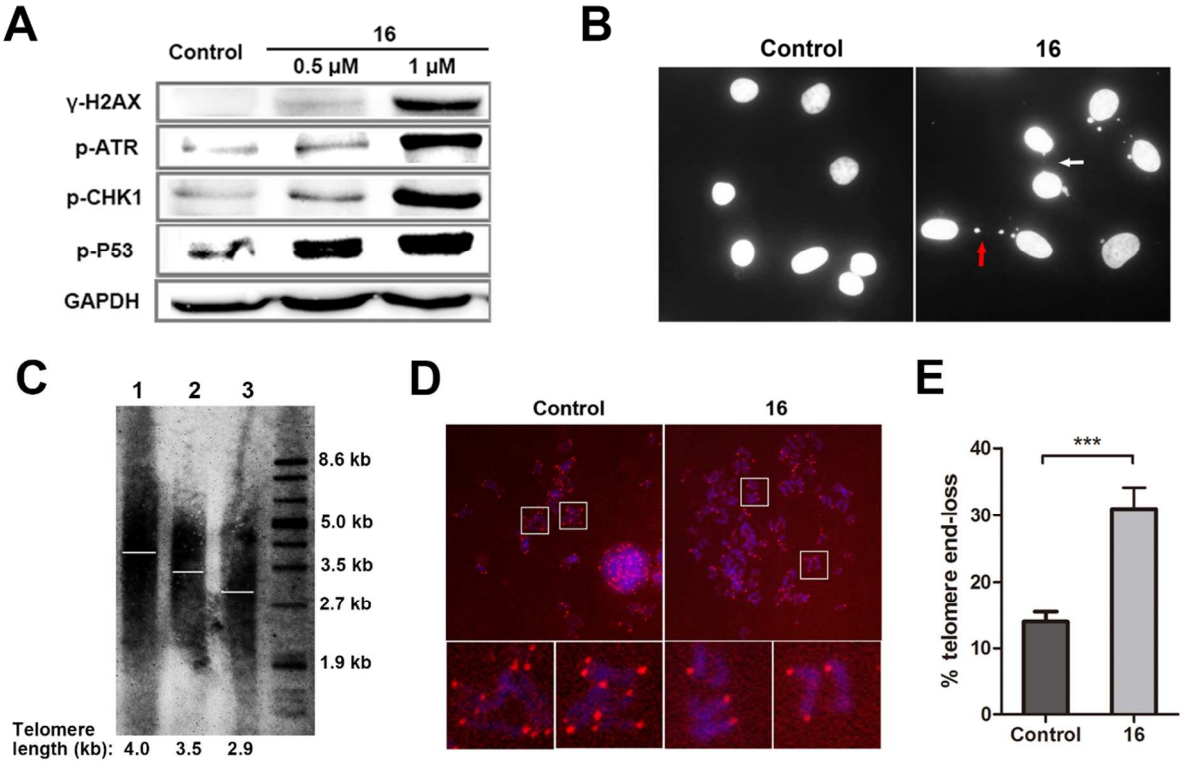

Figure 6. Compound **16** induced telomere shortening and telomere uncapping. (A) Expression of DNA damage response pathway-related proteins in SiHa cells. (B) Representative images of micronuclei and anaphase bridges in SiHa cells treated with 1 μM **16** for 48 h. The red arrow indicates a typical image of the micronucleus, and the white arrow indicates a typical image of the anaphase bridge formation. (C) TRF lengths measured in SiHa cells treated or untreated with **16** for 21 days. Lane 1, 0.1% DMSO; lane 2, 0.5 μM **16**; lane 3, 1 μM **16**. (D) Metaphase spreads from SiHa cells treated with 1 μM **16** or 0.1% DMSO for 48 h, analyzed by the telomeric FISH assay using a Tamra-OO-$[TTAGGG]_3$ PNA probe (red) and DAPI (blue). (E) Quantification of the telomere end-loss in SiHa cells. Two-tailed unpaired Student's t tests were applied for statistical analysis. The data were expressed as the mean ± SEM: (∗) $P < 0.05$, (∗∗) $P < 0.01$, and (∗∗∗) $P < 0.001$, significantly different from the control.

Telomeres can form a "cap" at the end of chromosomes, and alterations in the telomere protein binding may lead to telomere uncapping, with the formation of anaphase bridges and micronuclei.[51] As shown in Figure 6B, typical images of anaphase bridges (white arrow) and micronuclei (red arrow) were found in **16**-treated cells. In addition, studies have shown that the stabilization of telomeric G-quadruplex causing the telomeric DNA damage response may result in telomere shortening and telomere end-loss. Therefore, the telomere restriction fragment (TRF) assay was employed to detect the telomere length in untreated and **16**-treated SiHa cells. The results showed that the telomere length was significantly shorter in **16**-treated cells than in untreated cells after long-term proliferation (Figure 6C). To further detect the telomere on an individual chromosome, we performed the fluorescent in situ hybridization (FISH) assay. Telomeres (red dot) form tiny "caps" at the ends of chromosomes (blue), and one normal chromosome is protected by four telomeres. As shown in Figure 6D, the number of detectable telomeres (red dot) in **16**-treated cells was less than that in untreated cells. Quantitative analysis of the metaphase chromosomes showed that 31% ± 3% of chromosomes in **16**-treated cells had at least one telomere end-loss (Figure 6E).

Cell cycle arrest, apoptosis and antiproliferation evoked by 16-induced telomere dysfunction. Furthermore, we explored whether telomere dysfunction and the DNA damage response induced by **16** could result in cell cycle arrest and apoptosis. First, a flow cytometry assay determining the percentage of cells in each phase of the cell cycle was conducted. As shown in Figure 7A-B and Figure S16A-B, after a 12-h treatment, **16** induced a significant accumulation of cells in the G_2/M phase in both SiHa and U2OS cells. Compound **7** which showed poor activity toward telomeric G-quadruplex,

didn't affect cell cycle (Figure S17A-B). Annexin V-fluorescein isothiocyanate (Annexin V-FITC) and the propidium iodide (PI) staining assay were performed to evaluate apoptosis. As shown in Figure 7C-D and Figure S16C-D, **16** induced dose- dependent apoptotic cells death, and the population of apoptotic cells was approximately 60% after treatment with 2 μM **16**.

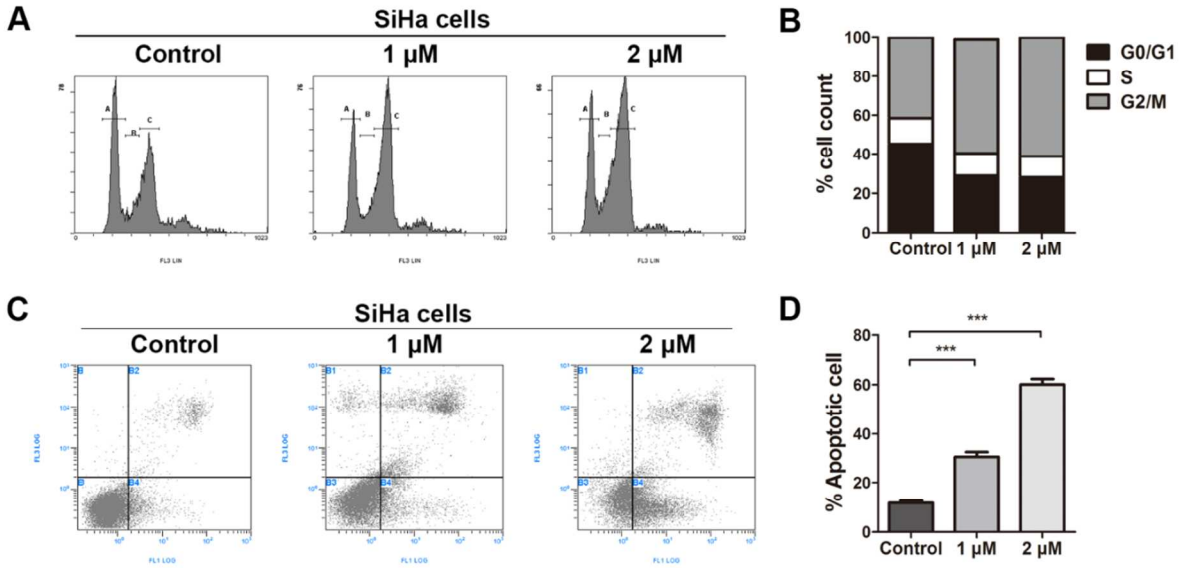

Figure 7. Compound **16** induced cell cycle arrest and apoptosis. (A) Cell cycle analysis after PI staining after a 12-h treatment with **16** or 0.1% DMSO in SiHa cells. (B) The percentage of SiHa cells in different phases of the cell cycle, analyzed by EXPO32 ADC software. (C) Apoptosis evaluation of SiHa cells after a 96-h treatment with **16**. The cells were collected and stained with Annexin V-FITC and PI. (D) The percentage of apoptosis in SiHa cells, analyzed by EXPO32 ADC software. The data were expressed as the mean ± SEM: (∗) $P < 0.05$, (∗∗) $P < 0.01$, and (∗∗∗) $P < 0.001$, significantly different from the control.

We also explored the antiproliferation activities of compound **16** in cells. Colony formation assays were performed to evaluate whether **16** reduced the tumorigenicity of SiHa cells. As shown in Figure S18A-B, after treatment with **16** for 12 days, colony formation obviously decreased. We also determined

the effects of the proliferation of SiHa cells using real-time cellular analysis (RTCA). The proliferation of SiHa cells was arrested in a dose-dependent manner after treatment with **16** for 90 h (Figure S18C). These results suggested that compound **16** could inhibit the proliferation of tumor cells.

Inhibition of tumor growth by compound 16 *in vivo*. Compound **16** presented effective antitumor activity *in vitro*, which prompted us to investigate its antitumor potential *in vivo*. We tested compound **16** in a SiHa xenograft mouse model of human cervical squamous cancer. SiHa tumors were established by subcutaneous injection of SiHa cells into the right armpit of in BALB/C-nu/nu mice. The mice were equally divided into four groups, the vehicle-treated group, the compound **16** (10 mg/kg)-treated group, the compound **16** (20 mg/kg)-treated group, and the doxorubicin (1.0 mg/kg)-treated group, n = 9/group, and treated via intraperitoneal (ip) injection daily. The tumors were collected after 3 weeks of treatment and analyzed. As shown in Figure 8A and 8B, the vehicle-treated group had an average tumor volume >1000 mm^3 after 21 days. In contrast, the tumor-bearing mice treated with compound **16** at 10 mg/kg and 20 mg/kg had an average tumor volume of < 800 mm^3 and < 400 mm^3, with a tumor growth inhibition rate of 29.0% and 65.2%, respectively (Figure 8C). Note that an obvious decrease in the mouse body weight was observed in the doxorubicin-treated group, but no significant change was observed in the **16**-treated group (Figure 8D). Altogether, these results demonstrated the compound **16** effectively inhibited tumor growth *in vivo*.

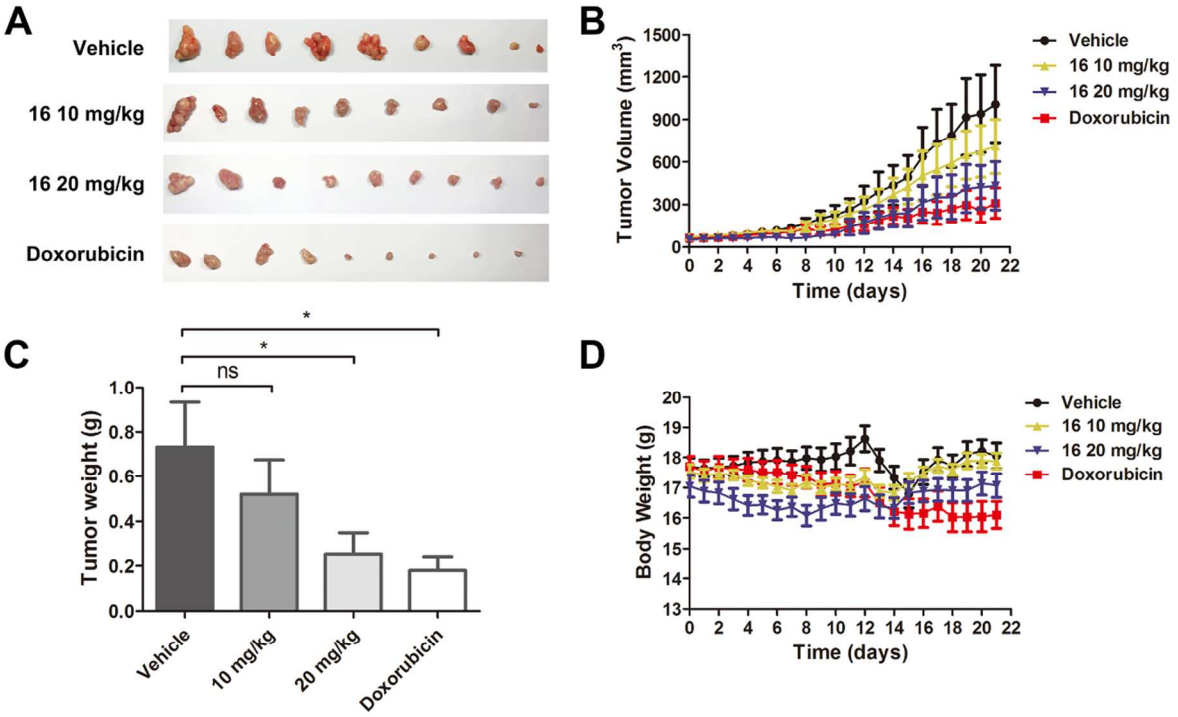

Figure 8. Compound **16** inhibits tumor growth in a Siha xenograft model *in vivo*. After treatment with **16** at 10 mg/kg or 20 mg/kg or doxorubicin at 1 mg/kg by ip injection for 3 weeks, the mice were sacrificed, and the tumors were weighed. (A) Images of excised tumors from each group. (B) Tumor volume of the mice in each group during the observation period. (C) Weights of the excised tumors from each group. (D) The body weight of the mice in each group during the observation period. The data are presented as means ± SEM, significantly different compared with the vehicle-treated group by the t-test, n = 9. The data were expressed as the mean ± SEM: (∗) $P < 0.05$, (∗∗) $P < 0.01$, and (∗∗∗) $P < 0.001$, significantly different from the control. (ns) Not significantly different from the control.

CONCLUSION

In this study, we designed and synthesized a series of new schizocommunin derivatives as potential telomeric G-quadruplex ligands. A panel of *in vitro* assays, including a FRET-melting experiment, a

competition FRET-melting experiment, a CD melting assay, and an SPR assay, were applied to evaluate the interaction between the derivatives and the telomeric G-quadruplex. Besides, the SARs were explored. Taken together, the results showed that most of derivatives displayed strong stabilization ability toward the telomeric G-quadruplex over duplex DNA, and the promising compound **16** was selected for the further study.

CD melting and SPR assays showed that **16** could interact with other G-quadruplex DNAs in some extent, but it was effective at stabilizing telomeric G-quadruplex. In addition, human telomeres feature a 3′-terminal single-stranded overhang TTAGGG repeats (~200 nt) and the copy numbers of telomeric G-quadruplex is larger than other G-quadruplexes in cells, so that it is more susceptible to be intervened by compounds. Notably, further cellar studies also proved that compound **16** could stabilize and induce the formation of the telomeric G-quadruplex, and triggered the DNA damage response at the telomeric region, thus inducing telomere uncapping and removal of telomere-binding proteins from the telomere, which result in telomere dysfunction and telomere shortening. These effects ultimately provoked p53-mediated cell cycle arrest and apoptosis, which is consistent with the behavior of an effective telomeric G-quadruplex ligand. In addition, **16** exhibited a potent anti-proliferation activity in cancer cell lines and a good antitumor ability via inhibition of cervical squamous cancer growth in BALB/C-nu/nu mice with a SiHa xenograft model. Collectively, these results proved that schizocommunin derivatives were a promising new class of telomeric G-quadruplex ligands.

EXPERIMENTAL SECTION

Chemical Synthesis

All chemicals were purchased from commercial sources unless otherwise specified. All the solvents were of analytical reagent grade and were used without further purification. ^{1}H and ^{13}C NMR spectra were recorded using tetramethylsilane (TMS) as the internal standard in DMSO-d_6, $CDCl_3$, Methanol-d_4 or Acetic acid-d_4 with a Bruker BioSpin GmbH spectrometer at 400 MHz and 101 MHz, respectively. Flash column chromatography was performed with silica gel (200-300 mesh) purchased from Qingdao Haiyang Chemical Co. Ltd. The purities of all compounds were confirmed to be higher than 95% by using analytical HPLC with a dual pump Shimadzu LC-20AB system equipped with an ZORBAX SB-C18 column (4.6×250 mm, 5 μm) and eluted with methanol/water (65:35) containing 0.1% TFA at a flow rate of 0.8 mL/min. Mass spectra (MS) were recorded on a Shimadzu LCMS-2010A instrument with an ESI or ACPI mass selective detector, and high-resolution mass spectra (HRMS) on Shimadzu LCMS-IT-TOF.

General method A for the preparation of the compounds 3a-3o. A mixture of **2a** or **2b** (1 equiv.), the respective amine (1.1 equiv.), anhydrous sodium carbonate (1.5 equiv.) and acetonitrile in pressure tubing was heated at 100°C for 24 h. The crude residue was adsorbed on silica and purified by flash chromatography.

7-((3-(dimethylamino)propyl)amino)-2-methylquinazolin-4(3*H*)-one (3a). Following general procedure A, intermediate **3a** was obtained from intermediate **2a** as white solid, yield 84%. ^{1}H NMR (400 MHz, $CDCl_3$) δ 11.78 (s, 1H), 7.99 (d, J = 8.7 Hz, 1H), 6.66 (d, J = 8.7 Hz, 1H), 6.63 (s, 1H), 5.56

(s, 1H), 3.29 (dd, *J* = 10.6, 5.7 Hz, 2H), 2.50 (s, 3H), 2.43 (t, *J* = 6.4 Hz, 2H), 2.26 (s, 6H), 1.86-1.77 (m, 2H).

6-fluoro-2-methyl-7-(4-methylpiperazin-1-yl)quinazolin-4(3*H*)-one (3b). Following general procedure A, intermediate **3b** was obtained from intermediate **2b** as white solid, yield 82%. ^{1}H NMR (400 MHz, CDCl3) δ 11.78 (s, 1H), 7.81 (d, *J* = 12.8 Hz, 1H), 7.10 (d, *J* = 7.8 Hz, 1H), 3.31 (t, *J* = 4.4 Hz, 4H), 2.63 (t, *J* = 4.4 Hz, 4H), 2.54 (s, 3H), 2.38 (s, 3H).

7-((2-(dimethylamino)ethyl)amino)-6-fluoro-2-methylquinazolin-4(3*H*)-one (3c). Following general procedure A, intermediate **3c** was obtained from intermediate **2b** as white solid, yield 73%. ^{1}H NMR (400 MHz, $CDCl_3$) δ 11.63 (s, 1H), 7.74 (d, *J* = 11.5 Hz, 1H), 6.75 (d, *J* = 7.7 Hz, 1H), 5.26 (t, *J* = 6.8 Hz, 1H), 3.26 (dd, *J* = 10.8, 5.3 Hz, 2H), 2.63 (t, *J* = 5.8 Hz, 2H), 2.52 (s, 3H), 2.28 (s, 6H).

7-((2-(diethylamino)ethyl)amino)-6-fluoro-2-methylquinazolin-4(3*H*)-one (3d). Following general procedure A, intermediate **3d** was obtained from intermediate **2b** as white solid, yield 63%. ^{1}H NMR (400 MHz, DMSO-d_6) *δ* 11.85 (s, 1H), 7.51 (d, *J* = 11.8 Hz, 1H), 6.67 (d, *J* = 8.0 Hz, 1H), 6.16 (t, *J* = 6.8 Hz, 1H), 3.23 (dd, *J* = 12.3, 6.2 Hz, 2H), 2.62 (t, *J* = 6.4 Hz, 2H), 2.56-2.51 (m, 4H), 2.27 (s, 3H), 0.97 (t, *J* = 7.1 Hz, 6H).

6-fluoro-2-methyl-7-((2-(pyrrolidin-1-yl)ethyl)amino)quinazolin-4(3*H*)-one (3e). Following general procedure A, intermediate **3e** was obtained from intermediate **2b** as white solid, yield 67%. ^{1}H NMR (400 MHz, DMSO-d_6) δ 11.85 (s, 1H), 7.51 (d, *J* = 11.8 Hz, 1H), 6.66 (d, *J* = 7.8 Hz, 1H), 6.27 (t, *J* = 6.8 Hz, 1H), 3.33-3.26 (m, 2H), 2.65 (t, *J* = 6.3 Hz, 2H), 2.51 (t, *J* = 6.8 Hz, 4H), 2.28 (s, 3H), 1.69 (t, *J* = 3.2 Hz, 4H).

6-fluoro-2-methyl-7-((2-(piperidin-1-yl)ethyl)amino)quinazolin-4(3*H*)-one (3f). Following general procedure A, intermediate **3f** was obtained from intermediate **2b** as white solid, yield 62%. ^{1}H NMR (400 MHz, DMSO-d_6) δ 11.84 (s, 1H), 7.51 (d, *J* = 11.8 Hz, 1H), 6.66 (d, *J* = 8.0 Hz, 1H), 6.18 (t, *J* = 6.8 Hz, 1H), 3.27 (dd, *J* = 12.3, 6.3 Hz, 2H), 2.53 (t, *J* = 6.2 Hz, 2H), 2.34-2.42 (m, 4H), 2.27 (s, 3H), 1.56-1.45 (m, 4H), 1.35-1.42 (m, 2H).

7-((3-(dimethylamino)propyl)amino)-6-fluoro-2-methylquinazolin-4(3*H*)-one (3g). Following general procedure A, intermediate **3g** was obtained from intermediate **2b** as white solid, yield 68%. ^{1}H NMR (400 MHz, $CDCl_3$) δ 11.48 (s, 1H), 7.74 (d, *J* = 11.5 Hz, 1H), 6.75 (d, *J* = 7.6 Hz, 1H), 6.13 (s, 1H), 3.35 (dd, *J* = 11.0, 5.6 Hz, 2H), 2.53 (s, 3H), 2.48 (t, *J* = 6.2 Hz, 2H), 2.29 (s, 6H), 1.87 (dt, *J* = 12.4, 6.1 Hz, 2H).

7-((3-(diethylamino)propyl)amino)-6-fluoro-2-methylquinazolin-4(3*H*)-one (3h). Following general procedure B, intermediate **3h** was obtained from intermediate **2b** as white solid, yield 73%. ^{1}H NMR (400 MHz, $CDCl_3$) δ 11.90 (s, 1H), 7.72 (d, *J* = 11.5 Hz, 1H), 6.93 (t, *J* = 6.8 Hz, 1H), 6.69 (d, *J* = 7.7 Hz, 1H), 3.32 (dd, *J* = 10.8, 5.7 Hz, 2H), 2.60 (t, *J* = 5.6 Hz, 2H), 2.57-2.51 (m, 4H), 2.52 (s, 3H), 1.85 (dt, *J* = 11.6, 5.6 Hz, 2H), 1.05 (t, *J* = 7.1 Hz, 6H).

6-fluoro-2-methyl-7-((3-(pyrrolidin-1-yl)propyl)amino)quinazolin-4(3*H*)-one (3i). Following general procedure A, intermediate **3i** was obtained from intermediate **2b** as white solid, yield 65%. ^{1}H NMR (400 MHz, DMSO-d_6) δ 11.83 (s, 1H), 7.49 (d, *J* = 11.8 Hz, 1H), 6.80 (t, *J* = 6.8 Hz, 1H), 6.64 (d, *J* = 8.0 Hz, 1H), 3.23 (dd, *J* = 12.3, 6.4 Hz, 2H), 2.53 (t, *J* = 6.8 Hz, 2H), 2.45 (t, *J* = 3.2 Hz, 4H), 2.27 (s, 3H), 1.82-1.72 (m, 2H), 1.70 (t, *J* = 3.2 Hz, 4H).

7-((3-(1*H*-imidazol-1-yl)propyl)amino)-6-fluoro-2-methylquinazolin-4(3*H*)-one (3j). Following general procedure A, intermediate **3j** was obtained from intermediate **2b** as white solid, yield 78%. ^{1}H NMR (400 MHz, DMSO-d_6) δ 7.67 (s, 1H), 7.52 (d, *J* = 11.8 Hz, 1H), 7.22 (s, 1H), 6.91 (s, 1H), 6.64 (d, *J* = 8.0 Hz, 1H), 6.59 (t, *J* = 6.8 Hz, 1H), 4.08 (t, *J* = 7.0 Hz, 2H), 3.15 (dd, *J* = 12.6, 6.5 Hz, 2H), 2.28 (s, 3H), 2.04 (dt, *J* = 14.0, 6.8 Hz, 2H).

6-fluoro-2-methyl-7-((3-morpholinopropyl)amino)quinazolin-4(3*H*)-one (3k). Following general procedure A, intermediate **3k** was obtained from intermediate **2b** as white solid, yield 80%. ^{1}H NMR (400 MHz, DMSO-d_6) δ 11.82 (s, 1H), 7.50 (d, *J* = 11.9 Hz, 1H), 6.75 (t, *J* = 6.8 Hz, 1H), 6.67 (d, *J* = 8.0 Hz, 1H), 3.60 (t, *J* = 5.2 ,4H), 3.23 (dd, *J* = 12.2, 6.3 Hz, 2H), 2.39 (m, 6H), 2.27 (s, 3H), 1.81-1.69 (m, 2H).

6-fluoro-2-methyl-7-((3-(4-methylpiperazin-1-yl)propyl)amino)quinazolin-4(3*H*)-one (3l). Following general procedure A, intermediate **3l** was obtained from intermediate **2b** as white solid, yield 65%. ^{1}H NMR (400 MHz, DMSO-d_6) δ 11.82 (s, 1H), 7.50 (d, *J* = 11.8 Hz, 1H), 6.78 (t, *J* = 6.8 Hz, 1H), 6.64 (d, *J* = 8.0 Hz, 1H), 3.22 (dd, *J* = 11.8, 6.1 Hz, 2H), 2.53 (t, *J* = 6.2 Hz, 2H), 2.45-2.36 (m, 8H), 2.27 (s, 3H), 2.19 (s, 3H), 1.82-1.64 (m, 2H).

7-(bis(3-(dimethylamino)propyl)amino)-6-fluoro-2-methylquinazolin-4(3*H*)-one (3m). Following general procedure A, intermediate **3m** was obtained from intermediate **2b** as white solid, yield 73%. ^{1}H NMR (400 MHz, $CDCl_3$) δ 11.62 (s, 1H), 7.78 (d, *J* = 11.5 Hz, 1H), 6.81 (d, *J* = 7.6 Hz, 1H), 3.38 (dd, *J* = 11.0, 5.6 Hz, 4H), 2.54 (s, 3H), 2.48 (t, *J* = 6.2 Hz, 4H), 2.32 (s, 12H), 1.86 (dt, *J* = 12.4, 6.1 Hz, 4H).

7-((3-(dimethylamino)propyl)amino)-6-fluoro-2,3-dimethylquinazolin-4(3*H*)-one (3n). Following general procedure A, intermediate **3n** was obtained from intermediate **2c** as white solid, yield 73%. ^{1}H NMR (400 MHz, $CDCl_3$) δ 7.71 (d, *J* = 11.7 Hz, 1H), 6.66 (d, *J* = 7.7 Hz, 1H), 5.95 (s, 1H), 3.57 (s, 3H), 3.31 (dd, *J* = 11.6, 5.9 Hz, 2H), 2.56 (s, 3H), 2.44 (t, *J* = 6.3 Hz, 2H), 2.26 (s, 6H), 1.84 (dt, *J* = 12.6, 6.3 Hz, 2H).

3-(3-(dimethylamino)propyl)-7-((3-(dimethylamino)propyl)amino)-6-fluoro-2-methylquinazolin-4(3*H*)-one (3o). Following general procedure A, intermediate **3o** was obtained from intermediate **2d** as white solid, yield 73%. ^{1}H NMR (400 MHz, $CDCl_3$) δ 7.68 (d, *J* = 8.2 Hz, 1H), 6.64 (d, *J* = 7.7 Hz, 1H), 6.09 (s, 1H), 4.09 (t, *J* = 7.6, 2H), 3.30 (dd, *J* = 11.6, 6.0 Hz, 2H), 2.61 (s, 3H), 2.43 (t, *J* = 6.3 Hz, 2H), 2.36 (t, *J* = 6.8 Hz, 2H), 2.25 (s, 6H), 2.24 (s, 6H), 1.93-1.79 (m, 4H).

General method B for the preparation of the compounds 6a-d. A mixture of **5a** or **5b** (1 equiv.), and the respective amine (1.1 equiv.) in acetonitrile was stirred at room temperature for 2~4 h. The crude residue was adsorbed on silica and purified by flash chromatography.

6-(4-methylpiperazin-1-yl)indoline-2,3-dione (6a). Following general procedure B, intermediate **6a** was obtained from intermediate **5a** as red solid, yield 58%. ^{1}H NMR (400 MHz, $CDCl_3$) δ 8.34 (s, 1H), 7.48 (d, *J* = 8.8 Hz, 1H), 6.43 (dd, *J* = 8.8, 2.1 Hz, 1H), 6.26 (d, *J* = 1.8 Hz, 1H), 3.52 (t, *J* = 5.2 Hz, 4H), 2.54 (t, *J* = 5.2 Hz, 4H), 2.35 (s, 3H).

5-fluoro-6-(4-methylpiperazin-1-yl)indoline-2,3-dione (6b). Following general procedure B, intermediate **6b** was obtained from intermediate **5b** as red solid, yield 48%. ^{1}H NMR (400 MHz, $CDCl_3$)

δ 8.30 (s, 1H), 7.23 (d, *J* = 12.1 Hz, 1H), 6.34 (d, *J* = 6.6 Hz, 1H), 3.43 (t, *J* = 5.2 Hz, 4H), 2.58 (t, *J* = 5.2 Hz, 4H), 2.36 (s, 3H).

5-fluoro-6-morpholinoindoline-2,3-dione (6c). Following general procedure B, intermediate **6c** was obtained from intermediate **5b** as red solid, yield 72%. ^{1}H NMR (400 MHz, DMSO-d_6) δ 10.84 (s, 1H), 7.32 (d, *J* = 12.4 Hz, 1H), 6.37 (d, *J* = 7.0 Hz, 1H), 3.74 (t, *J* = 4.8 Hz, 4H), 3.30 (t, *J* = 4.8 Hz, 4H).

6-((3-(dimethylamino)propyl)(methyl)amino)-5-fluoroindoline-2,3-dione (6d). Following general procedure B, intermediate **6d** was obtained from intermediate **5b** as red solid, yield 42%. ^{1}H NMR (400 MHz, $CDCl_3$) δ 7.15 (d, *J* = 13.4 Hz, 1H), 6.27 (d, *J* = 7.0 Hz, 1H), 3.52 (t, *J* = 7.3 Hz, 2H), 3.14 (d, *J* = 2.2 Hz, 3H), 2.40 (t, *J* = 7.0 Hz, 2H), 2.30 (s, 6H), 1.88 (dt, *J* = 14.4, 7.1 Hz, 2H).

1-(3-(diethylamino)propyl)indoline-2,3-dione (6e). A mixture of **5d** (1 equiv.), the ethylenediamine (1.1 equiv.) and anhydrous sodium carbonate (1.1 equiv.) in acetonitrile was stirred at room temperature for 2~4 h. The crude residue was adsorbed on silica and purified by flash chromatography as yellow oil, yield 67%. ^{1}H NMR (400 MHz, $CDCl_3$) δ 7.60-7.43 (m, 2H), 7.06 (t, *J* = 7.4 Hz, 1H), 6.98 (d, *J* = 7.9 Hz, 1H), 3.74 (t, *J* = 7.0 Hz, 2H), 2.75-2.49 (m, 6H), 2.14-1.78 (m, 2H), 1.04 (t, *J* = 7.0 Hz, 6H).

General method C for the preparation of the target compounds 7-37. A mixture of quinazolinone intermediates **3a-o** (1 equiv.) and isatin intermediates **5c**, **6a-6e** (1 equiv.) in acetic acid were refluxed for 8~12 h. The crude residue was adsorbed on silica and purified by flash

chromatography.

(Z)-7-((3-(dimethylamino)propyl)amino)-2-((2-oxoindolin-3-ylidene)methyl)quinazolin-4(3H)-one (7). Following general procedure C, compound **7** was obtained from intermediate **3a** and **5c** as yellow solid, yield 43%. ^{1}H NMR (400 MHz, DMSO-d_6) δ 13.89 (s, 1H), 11.44 (s, 1H), 7.90 (d, *J* = 7.5 Hz, 1H), 7.84 (d, *J* = 8.8 Hz, 1H), 7.47 (s, 1H), 7.36 (t, *J* = 7.6 Hz, 1H), 7.08 (t, *J* = 7.5 Hz, 1H), 6.93 (d, *J* = 7.6 Hz, 1H), 6.85 (d, *J* = 8.6 Hz, 1H), 6.78 (t, *J* = 4.4 Hz, 1H), 6.65 (s, 1H), 3.16 (dd, *J* = 11.8, 6.1 Hz, 2H), 2.33 (t, *J* = 6.5 Hz, 2H), 2.16 (s, 6H), 1.72 (dt, *J* = 13.7, 6.7 Hz, 2H). ^{13}C NMR (101 MHz, DMSO-d_6) δ 169.20, 160.66, 154.38, 151.64, 150.80, 141.99, 133.97, 131.86, 130.93, 127.32, 123.81, 122.93, 122.14, 115.72, 110.92, 110.46, 105.14, 57.19, 45.68, 40.96, 26.79. ESI-HRMS $[M+H]^+$ *m/z* = 390.1926, calcd for $C_{22}H_{23}N_5O_2$, 390.1925. Purity: 96.6% by HPLC.

(Z)-7-((3-(dimethylamino)propyl)amino)-6-fluoro-2-((2-oxoindolin-3-ylidene)methyl)quinazolin-4(3H)-one (8). Following general procedure C, compound **8** was obtained from intermediate **3g** and **5c** as yellow solid, yield 35%. ^{1}H NMR (400 MHz, Acetic-d_4) δ 7.43 (d, *J* = 11.5 Hz, 1H), 7.36 (d, *J* = 7.5 Hz, 1H), 7.25 (t, *J* = 7.6 Hz, 1H), 7.20 (s, 1H), 6.95 (t, *J* = 7.5 Hz, 1H), 6.87 (d, *J* = 7.7 Hz, 1H), 6.76 (d, *J* = 7.7 Hz, 1H), 3.40-3.34 (m, 2H), 3.26 (t, *J* = 6.5 Hz, 2H), 3.01 (s, 6H), 2.24-2.11 (m, 2H). ^{13}C NMR (101 MHz, Acetic-d_4) δ 168.75, 160.98 (d, *J* = 3.0 Hz), 151.27 (d, *J* = 248.4 Hz), 149.79, 146.79, 143.26 (d, *J* = 13.9 Hz), 141.04, 134.60, 131.76, 126.95, 123.10, 123.07, 121.37, 110.74, 109.84 (d, *J* = 20.9 Hz), 109.59 (d, *J* = 7.9 Hz), 104.89 (d, *J* = 3.3 Hz), 55.46, 42.67, 39.48, 23.09. ESI-HRMS $[M+H]^+$ *m/z* = 408.1828, calcd for $C_{22}H_{22}FN_5O_2$, 408.1830. Purity: 95.8% by HPLC.

(Z)-7-((3-(diethylamino)propyl)amino)-6-fluoro-2-((2-oxoindolin-3-ylidene)methyl)quinazolin

-4(3H)-one (9). Following general procedure C, compound **9** was obtained from intermediate **3h** and **5c** as yellow solid, yield 32%. ^{1}H NMR (400 MHz, DMSO-d_6) δ 14.06 (s, 1H), 11.43 (s, 1H), 7.87 (d, *J* = 7.3 Hz, 1H), 7.62 (d, *J* = 11.6 Hz, 1H), 7.44 (s, 1H), 7.35 (t, *J* = 7.6 Hz, 1H), 7.13-7.05 (m, 2H), 6.92 (d, *J* = 7.7 Hz, 1H), 6.80 (d, *J* = 7.6 Hz, 1H), 3.26 (t, *J* = 5.2 Hz, 2H), 2.53-2.45 (m, 6H), 1.84-1.65 (m, 2H), 0.98 (t, *J* = 7.0 Hz, 6H). ^{13}C NMR (101 MHz, Acetic-d_4) δ 168.84, 161.07 (d, *J* = 2.9 Hz), 151.34 (d, *J* = 248.2 Hz), 149.91, 146.88, 143.32 (d, *J* = 13.9 Hz), 141.11, 134.73, 131.79, 127.03, 123.15, 123.09, 121.40, 110.77, 109.89 (d, *J* = 20.4 Hz), 109.68 (d, *J* = 8.0 Hz), 104.89 (d, *J* = 3.8 Hz), 49.47, 46.74, 39.63, 22.55, 7.82. ESI-HRMS $[M+H]^+$ *m/z* = 436.2150, calcd for $C_{24}H_{26}FN_5O_2$, 436.2143. Purity: 96.0% by HPLC.

(Z)-6-fluoro-7-((3-morpholinopropyl)amino)-2-((2-oxoindolin-3-ylidene)methyl)quinazolin-4(3H)-one (10). Following general procedure C, compound **10** was obtained from intermediate **3k** and **5c** as yellow solid, yield 52%. ^{1}H NMR (400 MHz, DMSO-d_6) δ 14.05 (s, 1H), 11.44 (s, 1H), 7.86 (d, *J* = 7.6 Hz, 1H), 7.63 (d, *J* = 11.7 Hz, 1H), 7.42 (s, 1H), 7.35 (t, *J* = 7.7 Hz, 1H), 7.08 (t, *J* = 7.6 Hz, 1H), 6.92 (d, *J* = 7.6 Hz, 2H), 6.82 (d, *J* = 7.9 Hz, 1H), 3.64-3.53 (m, 4H), 3.30-3.24 (m, 2H), 2.46-2.34 (m, 6H), 1.83-1.73 (m, 2H). ^{13}C NMR (101 MHz, Acetic-d_4) δ 168.83, 161.05 (d, *J* = 2.8 Hz), 151.33 (d, *J* = 248.2 Hz), 149.85, 146.88, 143.29 (d, *J* = 13.6 Hz), 141.06, 134.63, 131.75, 127.11, 123.16, 123.07, 121.42, 110.72, 109.91 (d, *J* = 21.3 Hz), 109.69 (d, *J* = 7.9 Hz), 104.98 (d, *J* = 3.8 Hz), 63.81, 54.89, 51.76, 39.54, 22.21. ESI-HRMS $[M+H]^+$ *m/z* = 450.1930, calcd for $C_{24}H_{24}FN_5O_3$, 450.1936. Purity: 95.3% by HPLC.

(Z)-7-(bis(3-(dimethylamino)propyl)amino)-6-fluoro-2-((2-oxoindolin-3-ylidene)methyl)quinazolin-4(3H)-one (11). Following general procedure C, compound **11** was obtained from intermediate **3m** and **5c** as yellow solid, yield 40%. ^{1}H NMR (400 MHz, $CDCl_3$) δ 13.96 (s, 1H), 7.40 (dd, *J* = 18.8, 10.7 Hz, 2H), 7.26-7.21 (m, 1H), 7.09-6.99 (m, 3H), 6.70 (d, *J* = 7.7 Hz, 1H), 3.35 (t, *J* = 6.8 Hz, 4H), 2.40 (t, *J* = 7.2 Hz, 4H), 2.28 (s, 12H), 1.83 (dt, *J* = 13.7, 6.8 Hz, 4H). ^{13}C NMR (101 MHz, $CDCl_3$) δ 168.94, 160.61, 154.76, 151.16 (d, *J* = 223.6 Hz), 146.92, 143.44 (d, *J* = 9.8 Hz), 141.76, 133.71, 131.23, 128.98, 123.38, 122.55, 120.82, 114.68 (d, *J* = 3.2 Hz), 113.49 (d, *J* = 8.5 Hz), 112.41 (d, *J* = 24.9 Hz), 110.29, 56.63, 50.69, 44.98, 25.55. ESI-HRMS $[M+H]^+$ *m/z* = 493.2720, calcd for $C_{27}H_{33}FN_6O_2$, 493.2722. Purity: 95.1% by HPLC.

(Z)-7-((3-(dimethylamino)propyl)amino)-2-((6-(4-methylpiperazin-1-yl)-2-oxoindolin-3-ylidene)methyl)quinazolin-4(3H)-one (12). Following general procedure C, compound **12** was obtained from intermediate **3a** and **6a** as red solid, yield 27%. ^{1}H NMR (400 MHz, $CDCl_3$) δ 13.91 (s, 1H), 8.01 (d, *J* = 8.6 Hz, 1H), 7.30 (d, *J* = 8.2 Hz, 1H), 6.89 (s, 1H), 6.69 (d, *J* = 8.2 Hz, 1H), 6.68 (s, 1H), 6.46 (d, *J* = 8.6 Hz, 1H), 6.45 (s, 1H),3.32-3.22 (m, 6H), 2.51-2.43 (m, 6H), 2.30 (s, 9H), 1.85 (dt, *J* = 12.7, 6.3 Hz, 2H). ^{13}C NMR (101 MHz, $CDCl_3$) δ 170.09, 161.79, 153.62, 151.71, 151.04, 143.06, 133.40, 127.58, 124.75, 122.07, 115.64, 113.91, 111.02, 108.71, 105.18, 99.99, 97.21, 58.00, 54.50, 47.47, 45.96, 45.36, 42.54, 26.10. ESI-HRMS $[M+H]^+$ *m/z* = 488.2767, calcd for $C_{27}H_{33}N_7O_2$, 488.2768. Purity: 97.7% by HPLC.

(Z)-7-((2-(dimethylamino)ethyl)amino)-6-fluoro-2-((6-(4-methylpiperazin-1-yl)-2-oxoindolin-3-ylidene)methyl)quinazolin-4(3H)-one (13). Following general procedure C, compound **13** was

obtained from intermediate **3c** and **6a** as red solid, yield 21%. ^{1}H NMR (400 MHz, $CDCl_3$) δ 13.95 (s, 1H), 7.76 (d, *J* = 10.5 Hz, 1H), 7.30 (d, *J* = 14.4 Hz, 1H), 6.91 (s, 1H), 6.81 (d, *J* = 7.8 Hz, 1H), 6.56-6.38 (m, 2H), 3.35-3.20 (m, 6H), 2.66 (t, *J* = 7.2 Hz, 2H), 2.53 (t, *J* = 5.2 Hz, 4H), 2.34 (s, 3H), 2.31 (s, 6H). ^{13}C NMR (101 MHz, MeOD-d_4) δ 170.01, 161.64 (d, *J* = 2.4 Hz), 153.80, 151.22 (d, *J* = 247.4 Hz), 150.39, 148.23, 143.39, 143.20 (d, *J* = 13.9 Hz), 134.23, 123.48 (d, *J* = 8.8 Hz), 122.22, 113.91, 110.00 (d, *J* = 2.2 Hz), 109.79 (d, *J* = 2.7 Hz), 108.91, 105.84, 97.02, 57.13, 54.38, 47.26, 45.53, 44.80, 39.87. ESI-HRMS $[M+H]^+$ *m/z* = 492.2518, calcd for $C_{26}H_{30}FN_7O_2$, 492.2518. Purity: 95.5% by HPLC.

(Z)-6-fluoro-2-((6-(4-methylpiperazin-1-yl)-2-oxoindolin-3-ylidene)methyl)-7-((2-(pyrrolidin-1-yl)ethyl)amino)quinazolin-4(3H)-one (14). Following general procedure C, compound **14** was obtained from intermediate **3e** and **6a** as red solid, yield 16%. ^{1}H NMR (400 MHz, $CDCl_3$) δ 13.92 (s, 1H), 7.76 (d, *J* = 11.7 Hz, 1H), 7.35 (d, *J* = 8.4 Hz, 1H), 6.95 (s, 1H), 6.83 (d, *J* = 7.6 Hz, 1H), 6.54 (d, *J* = 8.3 Hz, 1H), 6.44 (s, 1H), 3.39-3.24 (m, 6H), 2.94-2.82 (m, 2H), 2.69-2.59 (m, 8H), 2.34 (s, 3H), 1.88-1.79 (m, 4H). ^{13}C NMR (101 MHz, MeOD-d_4) δ 170.04, 161.56, 153.78, δ 151.23 (d, *J* = 247.0 Hz), 150.37, 148.26, 143.23, 143.12, 134.02, 124.01, 122.23, 113.95, 110.14, 109.97, 108.95, 106.00, 97.04, 54.46, 54.17, 53.97, 47.42, 45.74, 41.28, 23.29. ESI-HRMS $[M+2H]^+$ *m/z* = 259.6382, calcd for $C_{28}H_{32}FN_7O_2$, 259.6374. Purity: 98.5% by HPLC.

(Z)-6-fluoro-2-((6-(4-methylpiperazin-1-yl)-2-oxoindolin-3-ylidene)methyl)-7-((2-(piperidin-1-yl)ethyl)amino)quinazolin-4(3H)-one (15). Following general procedure C, compound **15** was

obtained from intermediate **3f** and **6a** as red solid, yield 20%. ^{1}H NMR (400 MHz, $CDCl_3$) δ 14.00 (s, 1H), 7.73 (d, *J* = 11.4 Hz, 1H), 7.19 (d, *J* = 8.4 Hz, 1H), 6.79 (s, 1H), 6.75 (d, *J* = 7.6 Hz, 1H), 6.45 (s, 1H), 6.39 (d, *J* = 8.2 Hz, 1H), 3.32-3.20 (m, 6H), 2.70 (t, *J* = 7.2 Hz, 2H), 2.54-2.42 (m, 8H), 2.31 (s, 3H), 1.68-1.58 (m, 4H), 1.52-1.44 (m, 2H). ^{13}C NMR (101 MHz, MeOD-d_4) δ 169.98, 161.52, 153.71, 151.21 (d, *J* = 247.0 Hz), 150.32, 148.25, 143.23, 143.11, 133.95, 123.72, 122.14, 113.87, 110.05 (d, *J* = 6.0 Hz), 109.82, 108.83, 106.01 (d, *J* = 2.7 Hz), 97.00, 56.66, 54.39, 54.27, 47.29, 45.67, 39.19, 25.49, 23.99. HRMS $[M+H]^+$ *m/z* = 532.2826, calcd for $C_{29}H_{34}FN_7O_2$, 532.2831. Purity: 95.5% by HPLC.

(Z)-7-((3-(dimethylamino)propyl)amino)-6-fluoro-2-((6-(4-methylpiperazin-1-yl)-2-oxoindolin-3-yl idene)methyl)quinazolin-4(3H)-one (16). Following general procedure C, compound **16** was obtained from intermediate **3g** and **6a** as red solid, yield 31%. ^{1}H NMR (400 MHz, $CDCl_3$) δ 13.96 (s, 1H), 7.74 (d, *J* = 11.5 Hz, 1H), 7.31 (d, *J* = 8.6 Hz, 1H), 6.92 (s, 1H), 6.79 (d, *J* = 7.7 Hz, 1H), 6.51 (dd, *J* = 8.7, 2.1 Hz, 1H), 6.44 (d, *J* = 2.0 Hz, 1H), 5.95 (s, 1H), 3.40-3.25 (m, 6H), 2.56-2.43 (m, 6H), 2.33 (s, 3H), 2.29 (s, 6H), 1.88 (dt, *J* = 12.4, 6.2 Hz, 2H). ^{13}C NMR (101 MHz, MeOD-d_4) δ 169.93, 161.65 (d, *J* = 3.2 Hz), 153.77, 151.17 (d, *J* = 246.7 Hz), 150.34, 148.26, 143.50 (d, *J* = 13.8 Hz), 143.38, 134.18, 123.08, 122.09, 113.81, 109.63 (d, *J* = 20.9 Hz), 109.45 (d, *J* = 7.8 Hz), 108.81, 105.38 (d, *J* = 3.8 Hz), 96.76, 57.14, 54.28, 47.11, 45.36, 44.70, 41.15, 25.80. ESI-HRMS $[M+H]^+$ *m/z* = 506.2665, calcd for $C_{27}H_{32}FN_7O_2$, 506.2674. Purity: 99.9% by HPLC.

(Z)-7-((3-(diethylamino)propyl)amino)-6-fluoro-2-((6-(4-methylpiperazin-1-yl)-2-oxoindolin-3 -ylidene)methyl)quinazolin-4(3H)-one (17). Following general procedure C, compound **17** was

obtained from intermediate **3h** and **6a** as red solid, yield 28%. ^{1}H NMR (400 MHz, MeOD-d_4) δ 7.35 (d, J = 11.6 Hz, 1H), 7.09 (d, J = 8.6 Hz, 1H), 6.52 (d, J = 7.7 Hz, 1H), 6.45 (s, 1H), 6.33 (d, J = 7.5 Hz, 1H), 6.07 (s, 1H), 3.15 (t, J = 6.6 Hz, 2H), 3.08 (t, J = 5.2 Hz, 4H), 2.66-2.53 (m, 6H), 2.36 (t, J = 5.2 Hz, 4H), 2.20 (s, 3H), 1.78 (dt, J = 13.7, 6.6 Hz, 2H), 1.02 (t, J = 7.2 Hz, 6H). ^{13}C NMR (101 MHz, MeOD-d_4) δ 170.04, 161.75 (d, J = 2.5 Hz), 153.82, 151.34 (d, J = 247.2 Hz), 150.36, 148.34, 143.65 (d, J = 14.0 Hz), 143.41, 134.25, 123.53, 122.24, 113.94, 109.71 (d, J = 20.9 Hz), 109.51 (d, J = 7.9 Hz), 108.92, 105.43 (d, J = 4.1 Hz), 97.00, 54.38, 51.32, 47.28, 46.59, 45.55, 42.24, 24.83, 10.84. ESI-HRMS $[M+2H]^+$ m/z = 267.6519, calcd for $C_{29}H_{36}FN_7O_2$, 267.6530. Purity: 99.0% by HPLC.

(Z)-7-((2-(dimethylamino)ethyl)amino)-2-((6-((3-(dimethylamino)propyl)(methyl)amino)-5-fluoro-2-oxoindolin-3-ylidene)methyl)-6-fluoroquinazolin-4(3H)-one (18). Following general procedure C, compound **18** was obtained from intermediate **3c** and **6d** as red solid, yield 15%. ^{1}H NMR (400 MHz, DMSO-d_6) δ 14.00 (s, 1H), 11.24 (s, 1H), 7.70 (d, J = 13.8 Hz, 1H), 7.61 (d, J = 11.6 Hz, 1H), 7.20 (s, 1H), 6.79 (d, J = 8.0 Hz, 1H), 6.35 (d, J = 7.6 Hz, 1H), 6.32 (s, 1H), 3.32-3.25 (m, 6H), 2.90 (s, 3H), 2.25-2.17 (m, 4H), 2.22 (s, 6H), 2.11 (s, 6H), 1.74-1.60 (m, 2H). ^{13}C NMR (101 MHz, Acetic-d_4) δ 169.59, 161.08 (d, J = 4.6 Hz), 151.67 (d, J = 157.4 Hz), 149.26 (d, J = 145.8 Hz), 148.54, 146.63, 142.98 (d, J = 8.8 Hz), 142.66 (d, J = 13.3 Hz), 139.03, 134.66, 122.39, 113.07 (d, J = 9.1 Hz), 110.07 (d, J = 10.7 Hz), 109.94, 109.53 (d, J = 22.1 Hz), 104.92, 99.51, 55.40, 51.81, 43.00, 42.69, 38.74, 37.51, 22.88. ESI-HRMS $[M+2H]^+$ m/z = 263.6394, calcd for $C_{27}H_{33}F_2N_7O_2$, 263.6405. Purity: 99.9% by HPLC.

(Z)-2-((6-((3-(dimethylamino)propyl)(methyl)amino)-5-fluoro-2-oxoindolin-3-ylidene)methyl)-7-((3-(dimethylamino)propyl)amino)-6-fluoroquinazolin-4(3H)-one (19). Following general procedure C, compound **19** was obtained from intermediate **3g** and **6d** as red solid, yield 15%. ^{1}H NMR (400 MHz, $CDCl_3$) δ 14.01 (s, 1H), 7.73 (d, *J* = 11.4 Hz, 1H), 7.00 (d, *J* = 13.0 Hz, 1H), 6.82 (s, 1H), 6.77 (d, *J* = 7.7 Hz, 1H), 6.39 (d, *J* = 7.3 Hz, 1H), 6.00 (s, 1H), 3.41-3.21 (m, 4H), 2.93 (s, 3H), 2.48 (t, *J* = 6.3 Hz, 2H), 2.36 (t, *J* = 7.2 Hz, 2H), 2.29 (s, 6H), 2.27 (s, 6H), 1.87 (dt, *J* = 12.6, 6.2 Hz, 2H), 1.80 (dt, *J* = 14.4, 7.2 Hz, 2H). ^{13}C NMR (101 MHz, $CDCl_3$) δ 169.96, 161.09, 151.54 (d, *J* = 165.6 Hz), 150.09, 149.22 (d, *J* = 175.1 Hz), 148.31, 143.13 (d, *J* = 13.9 Hz), 142.56 (d, *J* = 9.2 Hz), 138.90, 133.25, 125.14, 112.63 (d, *J* = 9.1 Hz), 110.05 (d, *J* = 8.3 Hz), 109.83 (d, *J* = 20.6 Hz), 108.71 (d, *J* = 24.8 Hz), 106.16 (d, *J* = 4.4 Hz), 99.57 (d, *J* = 2.7 Hz), 58.07, 56.80, 45.33, 45.14, 42.52, 39.69, 29.70, 25.73, 25.60. ESI-HRMS $[M+H]^+$ *m/z* = 540.2902, calcd for $C_{28}H_{35}F_2N_7O_2$, 540.2893. Purity: 95.7% by HPLC.

(Z)-2-((6-((3-(dimethylamino)propyl)(methyl)amino)-5-fluoro-2-oxoindolin-3-ylidene)methyl)-6-fluoro-7-(4-methylpiperazin-1-yl)quinazolin-4(3H)-one (20). Following general procedure C, compound **20** was obtained from intermediate **3b** and **6d** as yellow solid, yield 23%. ^{1}H NMR (400 MHz, $CDCl_3$) δ 14.18 (s, 1H), 7.76 (d, *J* = 12.8 Hz, 1H), 7.11 (d, *J* = 7.8 Hz, 1H), 6.92 (d, *J* = 13.2 Hz, 1H), 6.75 (s, 1H), 6.40 (d, *J* = 7.3 Hz, 1H), 3.35-3.20 (m, 6H), 2.91 (s, 3H), 2.62 (t, *J* = 6.0 Hz, 4H), 2.38 (s, 3H), 2.34 (t, *J* = 7.2 Hz, 2H), 2.26 (s, 6H), 1.78 (dt, *J* = 14.2, 7.0 Hz, 2H). ^{13}C NMR (101 MHz, MeOD-d_4) δ 170.94, 161.99, 155.85, 149.80, 147.18, 146.30, 142.78, 134.51, 120.46, 117.69 (d, *J* = 27.7 Hz), 115.08 (d, *J* = 18.3 Hz), 112.08 (d, *J* = 4.9 Hz), 111.85 (d, *J* = 7.5 Hz), 111.49 (d, *J* = 10.6 Hz),

98.78, 55.63, 54.47, 45.31, 43.15, 39.13, 29.54, 23.64, 21.93. ESI-HRMS $[M+H]^+$ *m/z* = 538.2753, calcd for $C_{28}H_{33}F_2N_7O_2$, 538.2737. Purity: 99.2% by HPLC.

(Z)-7-((3-(dimethylamino)propyl)amino)-6-fluoro-2-((5-fluoro-6-morpholino-2-oxoindolin-3-ylidene)methyl)quinazolin-4(3H)-one (21). Following general procedure C, compound **8** was obtained from intermediate **3g** and **6c** as yellow solid, yield 42%. ^{1}H NMR (400 MHz, DMSO-d_6) δ 13.97 (s, 1H), 11.34 (s, 1H), 7.79 (d, *J* = 13.4 Hz, 1H), 7.61 (d, *J* = 12.0 Hz, 1H), 7.31 (s, 1H), 6.84-6.76 (m, 2H), 6.48 (s, 1H), 3.75 (t, *J* = 6.0 Hz, 4H), 3.30-3.21 (m, 2H), 3.09 (t, *J* = 6.0 Hz, 4H), 2.36 (t, *J* = 7.2 Hz, 2H), 2.19 (s, 6H), 1.75 (dt, *J* = 14.2, 7.0 Hz, 2H). ^{13}C NMR (101 MHz, Acetic-d_4) δ 169.44, 160.94, 152.45, 152.32, 150.00, 146.80, 143.46, 138.57, 134.40, 124.85, 115.56 (d, *J* = 9.1 Hz), 109.94 (d, *J* = 21.3 Hz), 109.56 (d, *J* = 11.0 Hz), 109.40 (d, *J* = 7.8 Hz), 104.45, 100.90, 66.29, 55.51, 50.10, 42.68, 39.54, 23.14. ESI-HRMS $[M+H]^+$ *m/z* = 511.2254, calcd for $C_{26}H_{28}F_2N_6O_3$, 511.2264. Purity: 95.2% by HPLC.

(Z)-7-((3-(diethylamino)propyl)amino)-6-fluoro-2-((5-fluoro-6-morpholino-2-oxoindolin-3-ylidene)methyl)quinazolin-4(3H)-one (22). Following general procedure C, compound **22** was obtained from intermediate **3h** and **6c** as yellow solid, yield 45%. ^{1}H NMR (400 MHz, $CDCl_3$) δ 13.99 (s, 1H), 7.62 (d, *J* = 11.4 Hz, 1H), 6.96 (d, *J* = 12.1 Hz, 1H), 6.85 (s, 1H), 6.78 (s, 1H), 6.70 (d, *J* = 7.7 Hz, 1H), 6.56 (d, *J* = 6.9 Hz, 1H), 3.81 (t, *J* = 6.0 Hz, 4H), 3.31 (t, *J* = 5.2 Hz, 2H), 3.12 (t, *J* = 6.0 Hz, 4H), 2.68-2.61 (t, *J* = 6.0 Hz, 2H), 2.57 (dd, *J* = 14.2, 7.1 Hz, 4H), 1.91-1.84 (m, 2H), 1.07 (t, *J* = 7.1 Hz, 6H). ^{13}C NMR (101 MHz, Acetic-d_4) δ 169.31, 160.95 (d, *J* = 3.4 Hz), 152.43 (d, *J* = 10.3 Hz), 150.09, 149.91, 148.33

(d, J = 325.5 Hz), 146.71, 143.44 (d, J = 9.4 Hz),143.23 (d, J = 13.8 Hz), 138.54, 134.34, 124.57, 115.40 (d, J = 9.2 Hz), 109.94-109.47 (m), 109.33 (d, J = 8.1 Hz), 104.55, 100.73, 66.29, 50.07, 49.53, 46.86, 39.66, 22.59, 7.89. ESI-HRMS $[M+H]^+$ m/z = 539.2574, calcd for $C_{28}H_{32}F_2N_6O_3$, 539.2577. Purity: 95.5% by HPLC.

(Z)-6-fluoro-2-((5-fluoro-6-morpholino-2-oxoindolin-3-ylidene)methyl)-7-((3-(pyrrolidin-1-yl) propyl)amino)quinazolin-4(3H)-one (23). Following general procedure C, compound **23** was obtained from intermediate **3i** and **6c** as yellow solid, yield 42%. ^{1}H NMR (400 MHz, DMSO-d_6) δ 13.97 (s, 1H), 11.35 (s, 1H), 7.77 (d, J = 12.7 Hz, 1H), 7.59 (d, J = 11.6 Hz, 1H), 7.29 (s, 1H), 6.97 (s, 1H), 6.77 (d, J = 7.8 Hz, 1H), 6.46 (d, J = 7.0 Hz, 1H), 3.75 (t, J = 5.4 Hz, 4H), 3.27 (dd, J = 11.5, 6.1 Hz, 2H), 3.09 (t, J = 5.4 Hz,4H), 2.58-2.50 (m, 6H), 1.83-1.76 (m, 2H), 1.75-1.68 (m, 4H). ^{13}C NMR (101 MHz, Acetic-d_4) δ 169.42, 161.09 (d, J = 8.9 Hz), 152.46, 151.37 (d, J = 240.5 Hz), 150.17, 149.99, 146.82, 143.39 (d, J = 24.3 Hz), 138.54, 134.35, 124.85, 115.53 (d, J = 9.0 Hz), 109.90 (d, J = 21.1 Hz), 109.52 (d, J = 13.7 Hz), 109.37, 104.67, 100.80, 66.29, 54.02, 52.89, 50.12, 39.61, 24.46, 22.90. ESI-HRMS $[M+H]^+$ m/z = 537.2441, calcd for $C_{28}H_{30}F_2N_6O_3$, 537.2420. Purity: 95.4% by HPLC.

(Z)-6-fluoro-2-((5-fluoro-6-morpholino-2-oxoindolin-3-ylidene)methyl)-7-((3-morpholinoprop yl) amino)quinazolin-4(3H)-one (24). Following general procedure C, compound **24** was obtained from intermediate **3k** and **6c** as yellow solid, yield 32%. ^{1}H NMR (400 MHz, DMSO-d_6) δ 13.97 (s, 1H), 11.33 (s, 1H), 7.78 (d, J = 12.8 Hz, 1H), 7.62 (d, J = 11.7 Hz, 1H), 7.30 (s, 1H), 6.91 (s, 1H), 6.79 (d, J = 7.9 Hz, 1H), 6.47 (d, J = 7.3 Hz, 1H), 3.75 (t, J = 4.4 Hz, 4H), 3.61 (t, J = 4.4 Hz, 4H), 3.29-3.25 (m, 2H), 3.10 (t, J = 4.4 Hz, 4H), 2.45-2.33 (m, 6H), 1.84-1.74 (m, 2H). ^{13}C NMR (101 MHz, Acetic-d_4) δ

169.59, 161.20, 152.30, 150.53, 150.09, 147.01, 143.46, 143.26, 138.58, 134.42, 125.25, 115.66, 110.01, 109.65, 109.37, 104.87, 100.90, 66.29, 63.79, 54.91, 51.73, 50.15, 39.61, 22.20. ESI-HRMS $[M+H]^+$ *m/z* = 553.2385, calcd for $C_{28}H_{30}F_2N_6O_4$, 553.2369. Purity: 98.1% by HPLC.

(Z)-6-fluoro-2-((5-fluoro-6-(4-methylpiperazin-1-yl)-2-oxoindolin-3-ylidene)methyl)-7-(4-methylpiperazin-1-yl)quinazolin-4(3H)-one (25). Following general procedure C, compound **25** was obtained from intermediate **3b** and **6b** as yellow solid, yield 18%. ^{1}H NMR (400 MHz, $CDCl_3$) δ 14.28 (s, 1H), 7.58 (d, *J* = 11.2 Hz, 1H), 7.04 (d, *J* = 6.4 Hz, 1H), 6.73-6.64 (m, 2H), 6.52 (s, 1H), 3.30 (t, *J* = 5.2 Hz, 4H), 3.24 (t, *J* = 5.2 Hz, 4H), 2.75-2.55 (m, 8H), 2.44 (s, 3H), 2.41 (s, 3H). ^{13}C NMR (101 MHz, MeOD-d_4) δ 169.44, 161.21 (d, *J* = 2.3 Hz), 156.01, 153.50, 152.51, 150.12, 147.16, 146.35 (d, *J* = 9.8 Hz), 143.33 (d, *J* = 9.7 Hz), 138.97, 134.29, 126.14, 115.46 (d, *J* = 11.4 Hz), 114.90 (d, *J* = 8.7 Hz), 111.89 (d, *J* = 23.9 Hz), 109.01 (d, *J* = 25.5 Hz), 100.87, 54.60, 54.54, 49.45, 49.41, 49.27, 49.23, 45.40. ESI-HRMS $[M+H]^+$ *m/z* = 522.2426, calcd for $C_{27}H_{29}F_2N_7O_2$, 522.2424. Purity: 98.0% by HPLC.

(Z)-7-((2-(dimethylamino)ethyl)amino)-6-fluoro-2-((5-fluoro-6-(4-methylpiperazin-1-yl)-2-oxoindolin-3-ylidene)methyl)quinazolin-4(3H)-one (26). Following general procedure C, compound **26** was obtained from intermediate **3c** and **6b** as yellow solid, yield 15%. ^{1}H NMR (400 MHz, DMSO-d_6) δ 14.00 (s, 1H), 11.30 (s, 1H), 7.76 (d, *J* = 12.7 Hz, 1H), 7.61 (d, *J* = 11.7 Hz, 1H), 7.29 (s, 1H), 6.80 (d, *J* = 7.9 Hz, 1H), 6.45 (d, *J* = 7.2 Hz, 1H), 6.32 (s, 1H), 3.30 (t, *J* = 6.2 Hz, 2H), 3.10 (t, *J* = 5.2 Hz, 4H), 2.50-2.44 (m, 6H), 2.23 (s, 3H), 2.21 (s, 6H). ^{13}C NMR (101 MHz, Acetic-d_4) δ 167.89, 159.92, 151.39 (d, *J* = 15.9 Hz), 148.92, 148.70, 146.07, 141.37 (d, *J* = 17.4 Hz), 140.48 (d, *J* = 10.8 Hz), 137.43 (d, *J*= 5.8 Hz), 132.76 (d, *J* = 8.5 Hz), 125.20, 115.47, 109.37, 108.85 (d, *J* = 20.4 Hz), 108.14 (d, *J* = 24.9 Hz),

104.46, 100.40 (d, J = 3.1 Hz), 53.98, 51.76, 45.81, 41.51, 36.32, 28.22. ESI-HRMS $[M+2H]^+$ m/z = 255.6239, calcd for $C_{26}H_{29}F_2N_7O_2$, 255.6248. Purity: 98.9% by HPLC.

(Z)-7-((2-(diethylamino)ethyl)amino)-6-fluoro-2-((5-fluoro-6-(4-methylpiperazin-1-yl)-2-oxoindolin-3-ylidene)methyl)quinazolin-4(3H)-one (27). Following general procedure C, compound **27** was obtained from intermediate **3d** and **6b** as red solid, yield 10%. ^{1}H NMR (400 MHz, $CDCl_3$) δ 14.08 (s, 1H), 7.65 (d, J = 11.3 Hz, 1H), 6.89 (d, J = 11.4 Hz, 1H), 6.80 (s, 1H), 6.76 (d, J = 7.6 Hz, 1H), 6.59 (d, J = 2.5 Hz, 1H), 3.32-3.14 (m, 6H), 2.82-2.54 (m, 10H), 2.45 (s, 3H), 1.06 (t, J = 7.1 Hz, 6H). ^{13}C NMR (101 MHz, Acetic-d_4) δ 169.25, 161.20 (d, J = 3.1 Hz), 152.61, 150.19 (d, J = 10.3 Hz), 150.02, 147.02, 143.42 (d, J = 13.6 Hz), 141.84 (d, J = 10.4 Hz), 138.55, 134.17, 125.87, 116.71 (d, J = 9.0 Hz), 109.99 (d, J = 22.2 Hz), 109.71, 109.57 (d, J = 7.9 Hz), 104.82 (d, J = 2.9 Hz), 101.73, 54.01, 53.15, 52.86, 47.10, 42.74, 39.59, 24.44, 22.88. ESI-HRMS $[M+H]^+$ m/z = 538.2733, calcd for $C_{28}H_{33}F_2N_7O_2$, 538.2737. Purity: 99.6% by HPLC.

(Z)-6-fluoro-2-((5-fluoro-6-(4-methylpiperazin-1-yl)-2-oxoindolin-3-ylidene)methyl)-7-((2-(pyrrolidin-1-yl)ethyl)amino)quinazolin-4(3H)-one (28). Following general procedure C, compound **28** was obtained from intermediate **3e** and **6b** as yellow solid, yield 8%. δ 13.97 (s, 1H), 7.66 (d, J = 11.7 Hz, 1H), 6.98 (s, 1H), 6.82-6.80 (m, 2H), 6.55 (d, J = 8.3 Hz, 1H), 3.36-3.23 (m, 6H), 2.89-2.82 (m, 2H), 2.65-2.57 (m, 8H), 2.40 (s, 3H), 1.86-1.75 (m, 4H). ^{13}C NMR (101 MHz, Acetic-d_4) δ 169.36, 161.13, 152.74 (d, J = 5.4 Hz), 150.30, 150.16, 146.94, 142.70 (d, J = 9.1 Hz), 141.89 (d, J = 3.3 Hz), 138.65, 134.38 (d, J = 3.0 Hz), 125.85, 116.78 (d, J = 8.5 Hz), 110.28 (d, J = 9.1 Hz), 109.60 (d, J = 22.4 Hz),

105.13 (d, *J* = 2.6 Hz), 101.85, 100.00, 54.22, 53.14, 52.76, 47.15, 42.72, 38.57, 22.84. ESI-HRMS $[M+2H]^+$ *m/z* = 268.6323, calcd for $C_{28}H_{31}F_2N_7O_2$, 268.6326. Purity: 98.6% by HPLC.

(Z)-6-fluoro-2-((5-fluoro-6-(4-methylpiperazin-1-yl)-2-oxoindolin-3-ylidene)methyl)-7-((2-(piperidin-1-yl)ethyl)amino)quinazolin-4(3H)-one (29). Following general procedure C, compound **29** was obtained from intermediate **3f** and **6b** as yellow solid, yield 16%. ^{1}H NMR (400 MHz, DMSO-d_6) δ 14.00 (s, 1H), 11.31 (s, 1H), 7.77 (d, *J* = 12.7 Hz, 1H), 7.61 (d, *J* = 11.5 Hz, 1H), 7.30 (s, 1H), 6.79 (d, *J* = 7.7 Hz, 1H), 6.45 (d, *J* = 7.1 Hz, 1H), 6.37 (s, 1H), 3.10 (t, *J* = 5.2 Hz, 4H), 2.50-2.40 (m, 12H), 2.23 (s, 3H), 1.51 (t, *J* = 5.2 Hz, 4H), 1.42-1.38 (m, 2H). ^{13}C NMR (101 MHz, MeOD-d_4) δ 169.53, 161.49, δ 152.69 (d, *J* = 4.5 Hz), 150.27, 149.89, 148.12, 143.42 (d, *J* = 4.2 Hz), 143.26 (d, *J* = 9.8 Hz), 138.83 (d, *J* = 5.0 Hz), 133.95 (d, *J* = 7.9 Hz), 126.70 (d, *J* = 10.3 Hz), 115.73 (d, *J* = 9.0 Hz), 110.20 (d, *J* = 5.6 Hz),109.94 (d, *J* = 20.7 Hz), 109.03 (d, *J* = 25.0 Hz), 106.13, 101.02, 56.70, 54.68, 54.28, 49.58, 49.55, 45.67, 39.24, 25.51, 24.02. ESI-HRMS $[M+H]^+$ *m/z* = 550.2757, calcd for $C_{29}H_{33}F_2N_7O_2$, 550.2737. Purity: 97.9% by HPLC.

(Z)-7-((3-(dimethylamino)propyl)amino)-6-fluoro-2-((5-fluoro-6-(4-methylpiperazin-1-yl)-2-oxoindolin-3-ylidene)methyl)quinazolin-4(3H)-one (30). Following general procedure C, compound **30** was obtained from intermediate **3g** and **6b** as yellow solid, yield 21%. ^{1}H NMR (400 MHz, Acetic-d_4) δ 7.52 (d, *J* = 11.4 Hz, 1H), 7.16 (s, 1H), 7.07 (d, *J* = 11.8 Hz, 1H), 6.78 (d, *J* = 7.3 Hz, 1H), 6.58 (d, *J* = 6.4 Hz, 1H), 3.83-2.73 (m, 2H), 3.67 (t, *J* = 8.5 Hz, 2H), 3.43-2.32 (m, 8H), 3.03 (s, 3H), 3.01 (s, 6H), 2.22 (dt, *J* = 12.4, 6.2 Hz, 2H). ^{13}C NMR (101 MHz, Acetic-d_4) δ 169.20, 161.40, 151.52 (d, *J* = 248.2 Hz), 150.32,

149.85 (d, *J* = 1.7 Hz), 148.19, 143.59 (d, *J* = 14.2 Hz), 143.28 (d, *J* = 10.0 Hz), 138.83, 133.93, 125.63, 115.77 (d, *J* = 9.0 Hz), 109.92 (d, *J* = 5.8 Hz), 109.74, 109.05 (d, *J* = 25.0 Hz), 105.80 (d, *J* = 4.1 Hz), 101.06, 54.30, 53.24, 48.82, 47.46, 45.52, 39.95, 25.12. ESI-HRMS $[M+H]^+$ *m/z* = 524.2584, calcd for $C_{27}H_{31}F_2N_7O_2$, 524.2580. Purity: 99.8% by HPLC.

(Z)-7-((3-(diethylamino)propyl)amino)-6-fluoro-2-((5-fluoro-6-(4-methylpiperazin-1-yl)-2-oxoindolin-3-ylidene)methyl)quinazolin-4(3H)-one (31). Following general procedure C, compound **31** was obtained from intermediate **3h** and **6b** as yellow solid, yield 25%. ^{1}H NMR (400 MHz, MeOD-d_4) δ 7.71 (d, *J* = 11.4 Hz, 1H), 7.24 (d, *J* = 12.0 Hz, 1H), 6.98 (s, 1H), 6.81 (d, *J* = 7.6 Hz, 1H), 6.50 (d, *J* = 7.0 Hz, 1H), 3.40-3.33 (m, 2H), 3.22 (t, *J* = 7.2 Hz, 4H), 2.86-2.76 (m, 6H), 2.66 (t, *J* = 7.2 Hz, 4H), 2.39 (s, 3H), 2.05-1.94 (m, 2H). ^{13}C NMR (101 MHz, MeOD-d_4) δ 169.57, 161.53, δ 152.74 (d, *J* = 8.2 Hz), 150.32, 149.85 (d, *J* = 1.7 Hz), 148.19, 143.59 (d, *J* = 14.2 Hz), 143.28 (d, *J* = 10.0 Hz), 138.83, 133.93, 126.79, 115.77 (d, *J* = 9.0 Hz), 109.92 (d, *J* = 5.8 Hz), 109.74, 109.05 (d, *J* = 25.0 Hz), 105.80 (d, *J* = 4.1 Hz), 101.06, 54.69, 51.35, 49.62, 49.57, 46.66, 45.64, 42.15, 24.70, 10.67. ESI-HRMS $[M+2H]^+$ *m/z* = 276.6474, calcd for $C_{29}H_{35}F_2N_7O_2$, 276.6483. Purity: 99.4% by HPLC.

(Z)-6-fluoro-2-((5-fluoro-6-(4-methylpiperazin-1-yl)-2-oxoindolin-3-ylidene)methyl)-7-((3-(pyrrolidin-1-yl)propyl)amino)quinazolin-4(3H)-one (32). Following general procedure C, compound **32** was obtained from intermediate **3i** and **6b** as yellow solid, yield 20%. ^{1}H NMR (400 MHz, $CDCl_3$) δ 13.99 (s, 1H), 7.67 (d, *J* = 11.0 Hz, 1H), 7.04 (d, *J* = 11.7 Hz, 1H), 6.88 (s, 1H), 6.76 (d, *J* = 7.7 Hz, 1H), 6.53 (d, *J* = 6.5 Hz, 1H), 6.35 (s, 1H), 3.34-3.32 (m, 2H), 3.23 (t, *J* = 7.2 Hz,4H), 2.79 (t, *J* = 5.2 Hz,2H),

2.71-2.57 (m, 8H), 2.39 (s, 3H), 2.01-1.92 (m, 2H), 1.89-1.83(m, 4H). ^{13}C NMR (101 MHz, $CDCl_3$) δ 169.48, δ 160.92 (d, *J* = 2.8 Hz), 150.04, 149.93, 148.18, 147.82 (d, *J* = 934.8 Hz), 143.09, 142.96, 138.74, 133.29, 126.98, 115.32 (d, *J* = 8.7 Hz), 110.32 (d, *J* = 7.6 Hz), 109.91 (d, *J* = 21.8 Hz), 108.28 (d, *J* = 24.6 Hz), 106.81, 101.74, 54.84, 50.96, 49.65, 46.57, 45.88, 40.13, 29.70, 11.79. ESI-HRMS $[M+H]^+$ *m/z* = 550.2737, calcd for $C_{29}H_{33}F_2N_7O_2$, 550.2737. Purity: 97.9% by HPLC.

(Z)-7-((3-(1H-imidazol-1-yl)propyl)amino)-6-fluoro-2-((5-fluoro-6-(4-methylpiperazin-1-yl)-2-oxoindolin-3-ylidene)methyl)quinazolin-4(3H)-one (33). Following general procedure C, compound **33** was obtained from intermediate **3j** and **6b** as yellow solid, yield 25%. ^{1}H NMR (400 MHz, DMSO-d_6) δ 14.00 (s, 1H), 11.31 (s, 1H), 7.77 (d, *J* = 12.7 Hz, 1H), 7.67 (s, 1H), 7.63 (d, *J* = 11.6 Hz, 1H), 7.30 (s, 1H), 7.22 (s, 1H), 6.91 (s, 1H), 6.75 (d, *J* = 7.8 Hz, 2H), 6.47 (d, *J* = 7.1 Hz, 1H), 4.09 (t, *J* = 6.7 Hz, 2H), 3.17 (dd, *J* = 11.6, 5.9 Hz, 2H), 3.11 (t, *J* = 7.2 Hz, 4H), 2.50 (t, *J* = 7.2 Hz, 4H), 2.23 (s, 3H), 2.13-1.93 (m, 2H). ^{13}C NMR (101 MHz, $CDCl_3$) δ 169.31, 160.89, 160.85, 152.67, 150.22, 150.10, 146.00, 143.70, 143.56, 143.33, 134.10, 131.65, 126.34, 125.48, 122.30, 120.61, 110.46, 110.31, 110.25, 109.94, 109.86, 105.69, 105.66, 58.20, 56.51, 45.35, 45.17, 43.13, 42.76, 29.70, 26.92, 25.61. ESI-HRMS $[M+H]^+$ *m/z* = 547.2378, calcd for $C_{28}H_{28}F_2N_8O_2$, 547.2376. Purity: 99.8% by HPLC.

(Z)-6-fluoro-2-((5-fluoro-6-(4-methylpiperazin-1-yl)-2-oxoindolin-3-ylidene)methyl)-7-((3-(4-methylpiperazin-1-yl)propyl)amino)quinazolin-4(3H)-one (34). Following general procedure C, compound **34** was obtained from intermediate **3l** and **6b** as red solid, yield 9%. ^{1}H NMR (400 MHz, $CDCl_3$) δ 14.14 (s, 1H), 7.62 (d, *J* = 11.3 Hz, 1H), 6.85 (d, *J* = 11.9 Hz, 1H), 6.77 (s, 1H), 6.70 (d, *J* = 7.6 Hz, 1H),

6.65 (s, 1H), 6.56 (d, *J* = 6.9 Hz, 1H), 3.30 (dd, *J* = 8.0, *J* = 4.5 Hz, 2H), 3.22 (t, *J* = 5.6 Hz, 4H), 2.68-2.60 (m, 6H), 2.59 (t, *J* = 5.6 Hz, 4H), 2.40 (s, 3H), 2.35 (s, 3H), 1.93-1.85 (m, 2H). ^{13}C NMR (101 MHz, Acetic-d_4) δ 169.38, δ 161.32 (d, *J* = 3.0 Hz), 152.71, 150.18 (d, *J* = 17.2 Hz), 147.20, 146.84 (d, *J* = 699.2 Hz), 143.51, 141.87 (d, *J* = 10.4 Hz), 138.56, 134.17, 126.25, 116.84 (d, *J* = 9.2 Hz), 110.11 (d, *J* = 22.3 Hz), 109.78, 109.61 (d, *J* = 18.8 Hz), 105.05, 101.79, 72.30, 62.55, 53.16, 50.21, 48.65, 42.74, 42.44, 39.45, 22.45. ESI-HRMS $[M+2H]^+$ *m/z* = 290.1528, calcd for $C_{30}H_{36}F_2N_8O_2$, 290.1537. Purity: 95.5% by HPLC.

(E)-7-((3-(dimethylamino)propyl)amino)-6-fluoro-3-methyl-2-((6-(4-methylpiperazin-1-yl)-2-oxoindolin-3-ylidene)methyl)quinazolin-4(3H)-one (35). Following general procedure C, compound **35** was obtained from intermediate **3n** and **6a** as yellow solid, yield 15%. ^{1}H NMR (400 MHz, $CDCl_3$) δ 7.97 (d, *J* = 8.9 Hz, 1H), 7.81 (d, *J* = 11.6 Hz, 1H), 7.19 (s, 1H), 6.75 (t, *J* = 7.9 Hz, 1H), 6.43 (d, *J* = 8.9 Hz, 1H), 6.36 (s, 1H), 6.09 (s, 1H), 3.68 (s, 3H), 3.37-3.26 (m, 6H), 2.58-2.51 (m, 4H), 2.48 (t, *J* = 6.2 Hz, 2H), 2.34 (s, 3H), 2.28 (s, 6H), 1.95-1.80 (m, 2H). ^{13}C NMR (101 MHz, Acetic-d_4) δ 171.29, δ 161.76 (d, *J* = 3.1 Hz), 152.52, 151.36 (d, *J* = 245.7 Hz), 150.14, 145.90, 144.96, 143.43 (d, *J* = 13.6 Hz), 133.80, 128.06, 120.78, 112.21, 110.44 (d, *J* = 21.6 Hz), 109.48 (d, *J* = 8.0 Hz), 109.05, 105.18 (d, *J* = 3.7 Hz), 98.12, 55.50, 52.68, 45.13, 42.58, 39.65, 31.11, 23.27. ESI-HRMS $[M+H]^+$ *m/z* = 520.2837, calcd for $C_{28}H_{34}FN_7O_2$, 520.2831. Purity: 98.5% by HPLC.

(E)-3-(3-(dimethylamino)propyl)-7-((3-(dimethylamino)propyl)amino)-6-fluoro-2-((2-oxoindolin-3-ylidene)methyl)quinazolin-4(3H)-one (36). Following general procedure C, compound **36** was obtained from intermediate **3o** and **5c** as yellow solid, yield 35%. ^{1}H NMR (400 MHz, $CDCl_3$) δ 8.33 (s,

1H), 7.82 (d, *J* = 11.6 Hz, 1H), 7.74 (d, *J* = 7.7 Hz, 1H), 7.60 (s, 1H), 7.25 (t, *J* = 7.6 Hz, 1H), 6.90 (t, *J* = 7.6 Hz, 1H), 6.85 (d, *J* = 7.8 Hz, 1H), 6.76 (d, *J* = 7.7 Hz, 1H), 6.22 (d, *J* = 2.7 Hz, 1H), 4.20 (t, *J* = 6.4 Hz, 2H), 3.32 (dd, *J* = 11.3, 5.9 Hz, 2H), 2.46 (t, *J* = 6.2 Hz, 2H), 2.37 (t, *J* = 6.9 Hz, 2H), 2.27 (s, 6H), 2.20 (s, 6H), 1.98-1.87 (m, 4H). ^{13}C NMR (101 MHz, $CDCl_3$) δ 169.31, 160.85, 152.67, 150.10, 146.00, 143.56, 143.33, 134.10, 131.65, 126.34, 125.48, 122.30, 120.61, 110.46, 110.31, 109.92, 105.66, 58.20, 56.51, 45.35, 45.17, 43.13, 42.76, 29.70, 26.92, 25.61. ESI-HRMS $[M+H]^+$ *m/z* = 550.2737, calcd for $C_{29}H_{33}F_2N_7O_2$, 550.2737. Purity: 99.2% by HPLC.

(Z)-2-((1-(3-(diethylamino)propyl)-2-oxoindolin-3-ylidene)methyl)-6-fluoro-7-(4-methylpiperazin-1-yl)quinazolin-4(3H)-one (37). Following general procedure C, compound **37** was obtained from intermediate **3a** and **6f** as yellow solid, yield 37%. ^{1}H NMR (400 MHz, $CDCl_3$) δ 14.40 (s, 1H), 7.92 (d, *J* = 12.8 Hz, 1H), 7.56 (d, *J* = 7.5 Hz, 1H), 7.39 (t, *J* = 7.7 Hz, 1H), 7.29 (s, 1H), 7.20 (d, *J* = 7.7 Hz, 1H), 7.13 (t, *J* = 7.5 Hz, 1H), 6.99 (d, *J* = 7.8 Hz, 1H), 3.90 (t, *J* = 7.1 Hz, 2H), 3.31 (t, *J* = 4.4 Hz, 4H), 2.68-2.54 (m, 10H), 2.38 (s, 2H), 2.04-1.90 (m, 2H), 1.07 (t, *J* = 6.7 Hz, 4H). ^{13}C NMR (101 MHz, $CDCl_3$) δ 166.96, 160.74, 155.06 (d, *J* = 252.7 Hz), 150.08, 147.11, 146.38 (d, *J* = 10.0 Hz), 142.45, 132.87, 131.49, 130.01, 123.22, 122.60, 120.70, 116.06 (d, *J* = 3.3 Hz), 115.94 (d, *J* = 8.7 Hz), 112.56 (d, *J* = 23.9 Hz), 109.39, 54.85, 50.24, 49.89, 49.85, 46.64, 46.11, 38.90, 25.14, 11.47. ESI-HRMS $[M+H]^+$ *m/z* = 519.2886, calcd for $C_{29}H_{35}FN_6O_2$, 519.2878. Purity: 98.9% by HPLC.

Biological Assay.

FRET assay. FRET assay was carried out on a real-time PCR apparatus following previously published procedures.[38-41] The labeled oligonucleotides F21T: 5′-FAM-d(GGG[TTAGGG]$_3$)-TAMRA-3′, F10T: 5′-FAM-dTATAGCTATA-HEG-TATAGCTATA-TAMRA-3′, HEG linker is [(-CH_2-CH_2-O-)$_6$]. Fluorescence melting curves were determined with a Roche LightCycler 2 real-time PCR machine, using a total reaction volume of 20 μL, with 0.2 μM of labeled oligonucleotide in Tris-HCl buffer (10 mM, pH 7.4) containing 60 mM KCl. Fluorescence readings with excitation at 470 nm and detection at 530 nm were taken at intervals of 1 °C over the range 37-99 °C, with a constant temperature being maintained for 30 s prior to each reading and the rate was 1 °C/min to ensure a stable value. The melting of the G-quadruplex was monitored alone or in the presence of various concentrations of compounds and/or of double stranded competitor ds26 (5′-CAATCGGATCGAATTCGATCCGATTG-3′). Final analysis of the data was carried out using Origin8.0 (OriginLab Corp.).

SPR assay. SPR measurements were performed on a ProteOn® XPR36 Protein Interaction Array System (Bio-Rad Laboratories, Hercules, CA) using a Neutr Avidin-coated NLC sensor chip. In a typical experiment, biotinylated HTG21 (5′-d(GGG[TTAGGG]$_3$)-3′), biotinylated pu22 (5′-d(TGAGGGTGGGGAGGGTGGGGAA)-3'), biotinylated c-kit1 (5′- d(AGGGAGGGCGCTGGGA GGAGGG)-3'), biotinylated bcl-2 (5′-d(GGGCGCGGGAGGAAGGGGGCGGG)-3') and hairpin DNA (5′- d(TATAGCTATA-HEG-TATAGCTATA)-3') were folded in a filtered and degassed running buffer (50 mM Tris-HCl, pH 7.4, 100 mM KCl). The DNA samples (200 nM) were then captured in flow cells by 2 times of loading to a signal intensity of ~1,000 RU, and a blank cell was set as a control. Ligand solutions (at 0.625, 1.25, 2.5, 5, 10, 20 and 40 μM) were prepared within the running buffer by serial

dilutions from stock solutions. Six groups of samples were injected simultaneously at a flow rate of 25 μL/min for 400 s for associating, followed by 300 s of disassociation at 25°C. The NLC sensor chip was regenerated with a short injection of 1 M KCl between consecutive measurements.[45] The final graphs were obtained by subtracting blank sensorgrams from the hairpin or quadruplexes sensorgrams. The data were analyzed with ProteOn® manager software, using equilibrium analysis.

Cell culture. The human acute leukemia cell HL-60, adenocarcinomic human alveolar basal epithelial cancer cell A549, human cervical cancer cell HeLa, human cervical squamous cancer cell SiHa, and human osteosarcoma cell U2OS were obtained from the American Type Culture Collection (ATCC, Rockville, MD) and preserved at our lab. HL-60 cells were cultured in a RPMI-1640 medium (Gibco, Carlsbad, CA) supplemented with 10% fetal bovine serum (Gibco, Carlsbad, CA), and other cell lines were grown in Dulbecco's modifed Eagle's medium (DMEM) (Gibco, Carlsbad, CA) supplemented with 10% fetal bovine serum. All cells were cultured with 5% CO_2 at 37°C.

MTT assay. Cells were seeded on 96-well plates (5.0×10^3 cells / well) and exposed to various concentrations of compounds. After 48 h treatment, 20 μL of 2.5 mg/mL MTT solution was added to each well, and the cells were further incubated for 4 h. The cells in each well were then treated with dimethyl sulfoxide (DMSO) (100 μL per well), and the optical density (OD) was recorded at 570 nm. All experiments were parallel performed in triplicate, and the IC_{50} values were derived from the mean OD values of the triplicate tests versus the drug concentration curves.

Immunofluorescence assay. Cells grown on glass coverslips were fixed in 4% paraformaldehyde/PBS for 15 min, then permeabilized with 0.5% triton-X100/PBS at 37°C for 30 min, and finally blocked with 5% goat serum/PBS at 37°C for 3 h. Immunofluorescence was proceeded using reference methods.[15,16] Following the protocol with the G-quadruplex antibody BG4 (80 ng/μL) at 37 °C for 3 h, and subsequently with anti-FLAG antibody (#2368, Cell Signaling Technology) and γ-H2AX antibody (#9718, Cell Signaling Technology), or TRF2 antibody (ab13579, Abcam) at 4 °C overnight. The glass coverslips were washed six times with blocking buffer and were then incubated with anti-rabbit Alexa 488-conjugated antibody (A21206, Life Technology), anti-mouse Alexa 555-conjugated antibody (A21427, Life Technology), and 2 μg/mL of 4,6-diamidino-2-phenyl indole (DAPI, Invitrogen) was diluted in 5% goat serum/PBS at 37°C for 3 h. The glass coverslips were again washed six times with blocking buffer, and then, digital images were recorded using an LSM710 microscope (Zeiss, GER) and analyzed with ZEN software.

Western blot assay. The cells treated with compounds or control medium were collected and lysed in RIPA lysis buffer (Bioteke, China), and the protein concentrations were determined using a BCA protein assay kit (Pierce, U.S.A.). In total, 20 μg of protein was resolved on a 10% SDS-PAGE and was transferred to 0.22 μm immobilon polyvinyl difluoride (PVDF) membranes. The blots were blocked with 3% BSA for 1 h at room temperature and then probed with primary antibodies (1: 1,000) at 4°C for 16 h. After five washes, the blots were subsequently incubated with the corresponding secondary antibodies (1: 2,000) for 2 h at room temperature. The protein bands were visualized using chemiluminescence substrate, and images were acquired using a Tanon-4200SF gel imaging system

(Shanghai, China). Antibodies to GAPDH (#5174, Cell Signaling Technology, MA, USA), Phospho-ATR (Ser428) (#5883, Cell Signaling Technology), Phospho-p53 (Ser15) (#9286, Cell Signaling Technology), Phospho-Histone H2A.X (Ser139) (#9718, Cell Signaling Technology), Phospho-Chk1 (Ser345) (#2348, Cell Signaling Technology), anti-rabbit IgG-HRP (#7074, Cell Signaling Technology), and anti-mouse IgG-HRP (#7076, Cell Signaling Technology) were used.

Anaphase bridge analysis. The cells were fixed in 2% formaldehyde/0.2% glutaraldehyde for 15 min at room temperature. The fixing solution was removed, and the cells were gently washed twice with PBS and then stained with 2 μg/mL of DAPI at 37°C for 3 h. The cells were washed with PBS twice, and digital images were recorded using LSM710 microscope (Zeiss, GER) and analyzed with ZEN software. The frequency of anaphase bridges was calculated as the ratio between cells exhibiting anaphase bridges and the total number of cells. A minimum of 50 anaphase cells were examined in each experiment.

Telomere Length Assay. Cells treated with compound **16** or DMSO were incubated for 21 days. DMEM was replaced and different concentrations of **16** were added every 3 days. Telomere length was measured by Telo TAGGG Telomere Length Assay Kit (Roche). Briefly, genomic DNA was digested with Hinf1/Rsa1 restriction enzymes. The digested DNA fragments were separated on 0.8% agarose gel, transferred to a nylon membrane, and the transferred DNA fixed on the wet blotting membrane by baking the membrane at 120 °C for 20 min. Membrane was hybridized with a DIG-labeled hybridization probe for telomeric repeats and incubated with anti-DIG-alkaline phosphatase. TRF was performed by

chemiluminescence detection.

FISH assay. FISH was performed as previously described.[16] Cy_3-labeled $(CCCTAA)_3$ PNA probe (Panagene, Korea) was used. Fluorescence of telomeres was digitally imaged on a Zeiss microscope with Cy_3/DAPI filters. The frequency of telomere-free ends was analyzed by statistical analysis.

Cell cycle analysis. For flow cytometric analysis of DNA content, SiHa or U2OS cells were plated in 6-well plates (2.0 × 105 cells) and incubated with compounds or DMSO for 12 h. At the end of the treatment, the cells were collected and washed twice with PBS. Next, the cells were harvested and fixed in ice-cold 70% ethanol overnight. The cells were pelleted and resuspended in a staining solution (50 μg/mL PI, 75 KU/mL RNase A in PBS) for 30 min at room temperature in dark. Cells were analyzed by flow cytometry using an EPICS XL flow cytometer (Beckman Coulter, USA). For each analysis, 10, 000 events were collected. The cell cycle distribution was analyzed by EXPO32 ADC software.

Annexin V-FITC/PI Apoptosis Detection. The cells treated with compounds or DMSO and were washed twice with PBS, and detected using the annexin V-FITC/PI apoptosis detection kit (Key GEN). Briefly, SiHa or U2OS cells were pelleted and resuspended in binding buffer. Annexin V-FITC and PI were added, and the cells were disturbed by gently vortexing the samples prior to incubation for 15 min in the dark. Emitted florescence was quantitated by Epics Elite flow cytometry (Beckman Coulter, USA). For each analysis, 10, 000 events were collected. The data was analyzed by EXPO32 ADC software.

Xenograft Animal Model and Drug Treatments. Female BALB/C-nu/nu mice (4 weeks old) were purchased from and housed at the Experimental Animal Center of Sun Yat-sen University (Guang Zhou, China) and maintained in pathogen-free conditions (12 h light-dark cycle at 24±1˚C with 60-70% humidity and provided with food and water ad libitum). SiHa cells were harvested during log-phase growth and were resuspended in FBS-free DMEM medium to the density of 1×10^7 cells per 100 μL. Six mice were injected subcutaneously in the right flank with 100 μL. The tumor implanted in mice grows into almost 100 mm^3 after 3 weeks of feeding. These tumors were divided into thirty-six parts and implanted in mice. Tumor growth was examined twice a week after implantation, until the tumor volume reached approximately 60 mm^3. The mice were randomly divided into four groups of nine mice and treated intraperitoneally (ip) with various regimens. Mice in the control group were treated with an equivalent volume of vehicle, the compound **16**-treated group at a dose of 10 or 20 mg/kg, and the doxorubicin-treated group at a dose of 1 mg/kg. The volume of the tumor mass was measured with an electronic caliper and calculated as $1/2 \times \text{length} \times \text{width}^2$ in mm^3. The tumors size and the body weight of the mice were measured every day after drug treatment, and growth curves were plotted using average tumor volume within each experimental group. After treatment for 3 weeks, tumor tissues are collected and tested for weight and volume.

Data Analysis. Data was presented as the mean ± standard deviation (SEM) of three independent experiments. Statistical analysis was performed using GraphPad Prism 5.03 software.

ACKNOWLEDGMENTS

We thank Dr. Shankar Balasubramanian (University of Cambridge, UK) for providing BG4 antibody (plasmid). And the Natural Science Foundation of China (81330077 and 21172272 for Z.-S.H., 21672268 for J.-H.T., and 21472252 for D.L.), the Natural Science Foundation of Guangdong Province (2017A030308003 for Z.-S.H. and 2015A030306004 for J.-H.T.), and Guangdong Provincial Key Laboratory of Construction Foundation (2011A060901014) for financial support of this study.

AUTHOR INFORMATION

Corresponding Author

*(Z.-S.H.) Tel.: 8620-39943056. E-mail: ceshzs@mail.sysu.edu.cn.

*(J.-H.T.) Tel.: 8620-39943053. E-mail: tanjiah@mail.sysu.edu.cn.

Notes

The authors declare no competing financial interest.

ABBREVIATIONS

DNA, deoxyribonucleic acid; NOE, nuclear overhauser effect; FRET, fluorescence resonance energy transfer; HEG, hexaethylene glycol; FAM, carboxyfluorescein; TAMRA, carboxytetramethylrhodamine; CD, circular dichroism; SAR, structure-activity relationship; SPR, surface plasmon resonance; MTT, methyl thiazolyl tetrazolium; ALT, alternative lengthening of telomeres; TRAP, telomeric repeat

amplification protocol; TRF2, telomeric repeat binding factors 2; γ-H_2AX, histone H2A.X; SEM, standard error of mean; POT1, protection of telomeres 1; DAPI, 4',6-diamidino-2-phenylindole; ChIP-seq, chromatin immunoprecipitation sequencing; DMSO, dimethylsulfoxide; PI, propidium iodide; FITC, fluorescein isothiocyanate; ATR, ataxia telangiectasia and Rad3-related; CHK1, checkpoint kinase 1; FISH, fluorescent in situ hybridization; TRF, telomere restriction fragment; RTCA, real-time cellular analysis; TMS, tetramethylsilane; DSB, double-strand break; ip, intraperitoneal; DMEM, Dulbecco's modifed Eagle's medium.

ANCILLARY INFORMATION

Supporting Information

Additional experimental results, ^{1}H and ^{13}C NMR spectra, HRMS and HPLC assay data for final compounds, and a CSV file of molecular formula strings are available free of charge via the Internet at http://pubs.acs.org.

REFERENCES

1. O'Sullivan, R. J.; Karlseder, J. Telomeres: protecting chromosomes against genome instability. *Nat. Rev. Mol. Cell Biol.* **2010**, *11*, 171-181.

2. de Lange, T. How telomeres solve the end-protection problem. *Science* **2009**, *326*, 948-952.

3. Verdun, R. E.; Karlseder, J. Replication and protection of telomeres. *Nature* **2007**, *447*, 924-931.

4. de Lange, T. T-loops and the origin of telomeres. *Nat. Rev. Mol. Cell Biol.* **2004**, *5*, 323-329.

5. de Lange, T. Shelterin: the protein complex that shapes and safeguards human telomeres. *Genes Dev.* **2005**, *19*, 2100-2110.

6. Neidle, S.; Parkinson, G. Telomere maintenance as a target for anticancer drug discovery. *Nat. Rev. Drug Discov.* **2002**, *1*, 383-393.

7. Patel, D. J.; Phan, A. T.; Kuryavyi, V. Human telomere, oncogenic promoter and 5'-UTR G-quadruplexes: diverse higher order DNA and RNA targets for cancer therapeutics. *Nucleic Acids Res.* **2007**, *35*, 7429-7455.

8. Smith, F. W.; Feigon, J. Quadruplex structure of oxytricha telomeric DNA oligonucleotides. *Nature* **1992**, *356*, 164-168.

9. Parkinson, G. N.; Lee, M. P.; Neidle, S. Crystal structure of parallel quadruplexes from human telomeric DNA. *Nature* **2002**, *417*, 876-880.

10. Biffi, G.; Tannahill, D.; Mccafferty, J.; Balasubramanian, S. Quantitative visualization of DNA G-quadruplex structures in human cells. *Nat. Chem.* **2013**, *5*, 182-186.

11. Burger, A. M.; Dai, F.; Schultes, C. M.; Reszka, A. P.; Moore, M. J.; Double, J. A.; Neidle, S. The G-quadruplex-interactive molecule BRACO-19 inhibits tumor growth, consistent with telomere targeting and interference with telomerase function. *Cancer Res.* **2005**, *65*, 1489-1496.

12. Phatak, P.; Cookson, J. C.; Dai, F.; Smith, V.; Gartenhaus, R. B.; Stevens, M. F.; Burger, A. M. Telomere uncapping by the G-quadruplex ligand RHPS4 inhibits clonogenic tumour cell growth in vitro and in vivo consistent with a cancer stem cell targeting mechanism. *Br. J. Cancer* **2007**, *96*, 1223-1233.

13. Gomez, D.; O'Donohue, M. F.; Wenner, T.; Douarre, C.; Macadre, J.; Koebel, P.; Giraud-Panis, M. J.; Kaplan, H.; Kolkes, A.; Shin-ya, K.; Riou, J. F. The G-quadruplex ligand telomestatin inhibits POT1 binding to telomeric sequences in vitro and induces GFP-POT1 dissociation from telomeres in human cells. *Cancer Res.* **2006**, *66*,

6908-6912.

14. Rizzo, A.; Salvati, E.; Porru, M.; D'Angelo, C.; Stevens, M. F.; D'Incalci, M.; Leonetti, C.; Gilson, E.; Zupi, G.; Biroccio, A. Stabilization of quadruplex DNA perturbs telomere replication leading to the activation of an ATR-dependent ATM signaling pathway. *Nucleic Acids Res.* **2009**, *37*, 5353-5364.

15. Hu, M.-H.; Chen, S.-B.; Wang, B.; Ou, T.-M.; Gu, L.-Q.; Tan, J.-H.; Huang, Z.-S. Specific targeting of telomeric multimeric G-quadruplexes by a new triaryl-substituted imidazole. *Nucleic Acids Res.* **2017**, *45*, 1606-1618.

16. Zheng, X.-H.; Mu, G.; Zhong, Y.-F.; Zhang, T.-P.; Cao, Q.; Ji, L.-N.; Zhao, Y.; Mao, Z.-W. Trigeminal star-like platinum complexes induce cancer cell senescence through quadruplex-mediated telomere dysfunction. *Chem. Commun.* **2016**, *52*, 14101-14104.

17. Zhou, G.; Liu, X.; Li, Y.; Xu, S.; Ma, C.; Wu, X.; Cheng, Y.; Yu, Z.; Zhao, G.; Chen, Y. Telomere targeting with a novel G-quadruplex-interactive ligand BRACO-19 induces T-loop disassembly and telomerase displacement in human glioblastoma cells. *Oncotarget* **2016**, *7*, 14925-14939.

18. Neidle, S. Human telomeric G-quadruplex: the current status of telomeric G-quadruplexes as therapeutic targets in human cancer. *FEBS. J.* **2010**, *277*, 1118-1125.

19. Tan, Z.; Tang, J.; Kan, Z.-Y.; Hao, Y.-H. Telomere G-quadruplex as a potential target to accelerate telomere shortening by expanding the incomplete end-replication of relomere DNA. *Curr. Top. Med. Chem.* **2015**, *15*, 1940-1946.

20. Islam, M. K.; Jackson, P. J.; Rahman, K. M.; Thurston, D. E. Recent advances in targeting the telomeric G-quadruplex DNA sequence with small molecules as a strategy for anticancer therapies. *Future Med. Chem.* **2016**, *8*, 1259-1290.

21. Chauhan, A.; Paul, R.; Debnath, M.; Bessi, I.; Mandal, S.; Schwalbe, H.; Dash, J. Synthesis of fluorescent

binaphthyl amines that bind c-MYC G-Quadruplex DNA and repress c-MYC expression. *J. Med. Chem.* **2016**, *59*, 7275-7281.

22. Debnath, M.; Ghosh, S.; Chauhan, A.; Paul, R.; Bhattacharyya, K.; Dash, J. Preferential targeting of i-motifs and G-quadruplexes by small molecules. *Chem. Sci.* **2017**, *8*, 7448-7456.

23. Neidle, S. Quadruplex nucleic acids as novel therapeutic targets. *J. Med. Chem.* **2016**, 59, 5987-6011.

24. Rodrigues, T.; Reker, D.; Schneider, P.; Schneider, G. Counting on natural products for drug design. *Nat. Chem.* **2016**, *8*, 531-541.

25. Zhou, J.-L.; Lu, Y.-J.; Ou, T.-M.; Zhou, J.-M.; Huang, Z.-S.; Zhu, X.-F.; Du, C.-J.; Bu, X.-Z.; Ma, L.; Gu, L.-Q.; Li, Y.-M.; Chan, A.-S. Synthesis and evaluation of quindoline derivatives as G-quadruplex inducing and stabilizing ligands and potential inhibitors of telomerase. *J. Med. Chem.* **2005**, *48*, 7315-7321.

26. Rodriguez, R.; Muller, S.; Yeoman, J. A.; Trentesaux, C.; Riou, J. F.; Balasubramanian, S. A novel small molecule that alters shelterin integrity and triggers a DNA-damage response at telomeres. *J. Am. Chem. Soc.* **2008**, *130*, 15758-15759.

27. Hosoe, T.; Nozawa, K.; Kawahara, N.; Fukushima, K.; Nishimura, K.; Miyaji, M.; Kawai, K. Isolation of a new potent cytotoxic pigment along with indigotin from the pathogenic basidiomycetous fungus Schizophyllum commune. *Mycopathologia* **1999**, *146*, 9-12.

28. Uehata, K.; Kimura, N.; Hasegawa, K.; Arai, S.; Nishida, M.; Hosoe, T.; Kawai, K.; Nishida, A. Total synthesis of schizocommunin and revision of its structure. *J. Nat. Prod.* **2013**, *76*, 2034-2039.

29. Hou, J.-Q.; Tan, J.-H.; Wang, X.-X.; Chen, S.-B.; Huang, S.-Y.; Yan, J.-W.; Chen, S.-H.; Ou, T.-M.; Luo, H.-B.; Li, D.; Gu, L.-Q.; Huang, Z.-S. Impact of planarity of unfused aromatic molecules on G-quadruplex binding: learning from isaindigotone derivatives. *Org. Biomol. Chem.* **2011**, *9*, 6422-6436.

30. Li, Z.; Tan, J.-H.; He, J.-H.; Long, Y.; Ou, T.-M.; Li, D.; Gu, L.-Q.; Huang, Z.-S. Disubstituted quinazoline derivatives as a new type of highly selective ligands for telomeric G-quadruplex DNA. *Eur. J. Med. Chem.* **2012**, *47*, 299-311.

31. Hagmann, W. K. The many roles for fluorine in medicinal chemistry. *J. Med. Chem.* **2008**, *51*, 4359-4369.

32. Lu, Y.-J.; Ou, T.-M.; Tan, J.-H.; Hou, J.-Q.; Shao, W.-Y.; Peng, D.; Sun, N.; Wang, X.-D.; Wu, W.-B.; Bu, X.-Z.; Huang, Z.-S.; Ma, D.-L.; Wong, K.-Y.; Gu, L.-Q. 5-N-methylated quindoline derivatives as telomeric G-quadruplex stabilizing ligands: effects of 5-N positive charge on quadruplex binding affinity and cell proliferation. *J. Med. Chem.* **2008**, *51*, 6381-6392.

33. Okano, M.; Mito, J.; Maruyama, Y.; Masuda, H.; Niwa, T.; Nakagawa, S.; Nakamura, Y.; Matsuura, A. Discovery and structure-activity relationships of 4-aminoquinazoline derivatives, a novel class of opioid receptor like-1 (ORL1) antagonists. *Bioorg. Med. Chem.* **2009**, *17*, 119-132.

34. Shan, C.; Yan, J.-W.; Wang, Y.-Q.; Che, T.; Huang, Z.-L.; Chen, A.-C.; Yao, P.-F.; Tan, J.-H.; Li, D.; Ou, T.-M.; Gu, L.-Q.; Huang, Z.-S. Design, synthesis, and evaluation of isaindigotone derivatives to downregulate c-myc transcription via disrupting the Interaction of NM23-H2 with G-Quadruplex. *J. Med. Chem.* **2017**, *60*, 1292-1308.

35. Ranjit, K.; Rao, G. K.; Pai, P. N. S. Synthesis and biological evaluation of N1-[(3z)-5-substituted-2-oxo-1, 2-dihydro-3H-indol-3-ylidene]-5H-dibenzo [b,f] azepine-5-carbohydrazides. *International Journal of Biological Chemistry* **2010**, *4*, 19-26.

36. Singh, P.; Kaur, S.; Kumar, V.; Bedi, P. M.; Mahajan, M. P.; Sehar, I.; Pal, H. C.; Saxena, A. K. Synthesis and in vitro cytotoxic evaluation of N-alkylbromo and N-alkylphthalimido-isatins. *Bioorg. Med. Chem. Lett.* **2011**, *21*, 3017-3020.

37. Mergny, J. L.; Lacroix, L.; Teulade-Fichou, M. P.; Hounsou, C.; Guittat, L.; Hoarau, M.; Arimondo, P. B.;

Vigneron, J. P.; Lehn, J. M.; Riou, J. F.; Garestier, T.; Helene, C. Telomerase inhibitors based on quadruplex ligands selected by a fluorescence assay. *Proc. Natl. Acad. Sci. U. S. A.* **2001**, *98*, 3062-3067.

38. De Cian, A.; Guittat, L.; Kaiser, M.; Sacca, B.; Amrane, S.; Bourdoncle, A.; Alberti, P.; Teulade-Fichou, M. P.; Lacroix, L.; Mergny, J. L. Fluorescence-based melting assays for studying quadruplex ligands. *Methods* **2007**, *42*, 183-195.

39. Rachwal, P. A.; Fox, K. R. Quadruplex melting. *Methods* **2007**, *43*, 291-301.

40. Tan, J.-H.; Ou, T.-M.; Hou, J.-Q.; Lu, Y.-J.; Huang, S.-L.; Luo, H.-B.; Wu, J.-Y.; Huang, Z.-S.; Wong, K.-Y.; Gu, L.-Q. Isaindigotone derivatives: a new class of highly selective ligands for telomeric G-quadruplex DNA. *J. Med. Chem.* **2009**, *52*, 2825-2835.

41. Rezler, E. M.; Seenisamy, J.; Bashyam, S.; Kim, M. Y.; White, E.; Wilson, W. D.; Hurley, L. H. Telomestatin and diseleno sapphyrin bind selectively to two different forms of the human telomeric G-quadruplex structure. *J. Am. Chem. Soc.* **2005**, *127*, 9439-9447.

42. Nguyen, B.; Tanious, F. A.; Wilson, W. D. Biosensor-surface plasmon resonance: quantitative analysis of small molecule-nucleic acid interactions. *Methods* **2007**, *42*, 150-161.

43. Mosmann, T. J. Rapid colorimetric assay for cellular growth and survival: application to proliferation and cytotoxicity assays. *J. Immunol. Methods* **1983**, *65*, 55-63.

44. Reed, J.; Gunaratnam, M.; Beltran, M.; Reszka, A. P.; Vilar, R.; Neidle, S. TRAP-LIG, a modified telomere repeat amplification protocol assay to quantitate telomerase inhibition by small molecules. *Anal. Biochem.* **2008**, *380*, 99-105.

45. De Cian, A.; Cristofari, G.; Reichenbach, P.; De Lemos, E.; Monchaud, D.; Teulade-Fichou, M. P.; Shin-Ya, K.; Lacroix, L.; Lingner, J.; Mergny, J. L. Reevaluation of telomerase inhibition by quadruplex ligands and their

mechanisms of action. *Proc. Natl. Acad. Sci. U. S. A.* **2007**, *104*, 17347-17352.

46. Chen, Z.; Zheng, K.-W.; Hao, Y.-H.; Tan, Z. Reduced or diminished stabilization of the telomere G-quadruplex and inhibition of telomerase by small chemical ligands under molecular crowding condition. *J. Am. Chem. Soc.* **2009**, *131*, 10430-10438.

47. Hansel-Hertsch, R.; Beraldi, D.; Lensing, S. V.; Marsico, G.; Zyner, K.; Parry, A.; Di Antonio, M.; Pike, J.; Kimura, H.; Narita, M.; Tannahill, D.; Balasubramanian, S. G-quadruplex structures mark human regulatory chromatin. *Nat. Genet.* **2016**, *48*, 1267-1272.

48. Takai, H.; Smogorzewska, A.; de Lange, T. DNA damage foci at dysfunctional telomeres. *Current Biology* **2003**, *13*, 1549-1556.

49. Gomez, D.; Wenner, T.; Brassart, B.; Douarre, C.; O'Donohue, M. F.; El Khoury, V.; Shin-Ya, K.; Morjani, H.; Trentesaux, C.; Riou, J. F. Telomestatin-induced telomere uncapping is modulated by POT1 through G-overhang extension in HT1080 human tumor cells. *J. Biol. Chem.* **2006**, *281*, 38721-38729.

50. Guo, X.; Deng, Y.; Lin, Y.; Cosme-Blanco, W.; Chan, S.; He, H.; Yuan, G.; Brown, E. J.; Chang, S. Dysfunctional telomeres activate an ATM-ATR-dependent DNA damage response to suppress tumorigenesis. *EMBO. J.* **2007**, *26*, 4709-4719.

51. Wang, J.; Chen, Y.; Ren, J.; Zhao, C.; Qu, X. G-Quadruplex binding enantiomers show chiral selective interactions with human telomere. *Nucleic Acids Res.* **2014**, *42*, 3792-3802.

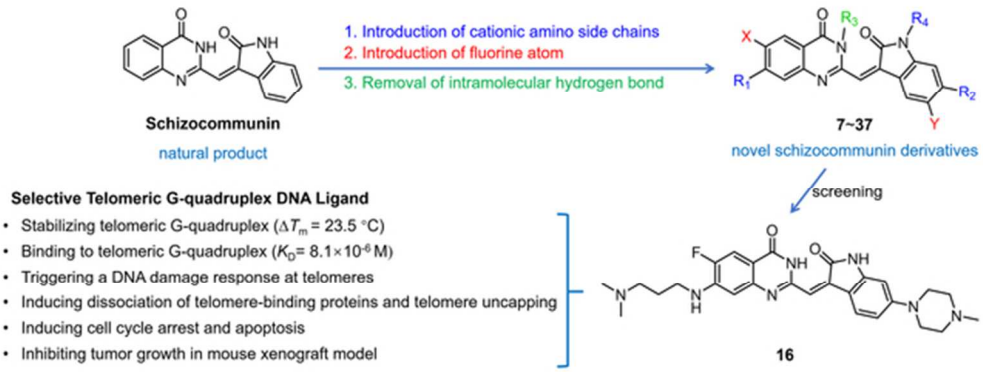

Table of Contents Graphic

54x21mm (300 x 300 DPI)